

Error estimates for a surface finite element method for anisotropic mean curvature flow

Klaus Deckelnick · Harald Garcke ·
Balázs Kovács

August 5, 2025

Abstract Error estimates are proved for an evolving surface finite element semi-discretization for anisotropic mean curvature flow of closed surfaces. For the geometric surface flow, a system coupling the anisotropic evolution law to parabolic evolution equations for the surface normal and normal velocity is derived, which then serve as the basis for the proposed numerical method. The algorithm for anisotropic mean curvature flow is proved to be convergent in the H^1 -norm with optimal-order for finite elements of degree at least two. Numerical experiments are presented to illustrate and complement our theoretical results.

1 Introduction

In this paper we propose an evolving surface finite element semi-discretization of anisotropic mean curvature flow for closed surfaces Γ (of dimension at most three). We prove optimal-order H^1 -norm error estimates for finite elements of degree at least two, and over time intervals on which the surface evolving under the anisotropic mean curvature flow remains sufficiently regular.

The proposed algorithm is based on a system coupling the anisotropic surface flow to parabolic evolution equations for the surface normal ν and normal velocity V . These equations are for the first time derived here. This approach was pioneered in 1984 by Huisken [Hui84] for mean curvature flow, and stays

Klaus Deckelnick

Institut für Analysis und Numerik, Otto-von-Guericke-Universität Magdeburg, Universitätsplatz 2, 39106 Magdeburg, Germany; E-mail: klaus.deckelnick@ovgu.de

H. Garcke

Faculty of Mathematics, University of Regensburg, Universitätsstr. 31, 93040 Regensburg, Germany; E-mail: harald.garcke@ur.de

B. Kovács

Institute of Mathematics, Paderborn University, Warburgerstr. 100., 31098 Paderborn, Germany; E-mail: balazs.kovacs@math.uni-paderborn.de

to be an important tool for the analysis of geometric flows ever since. The same idea has also been proved to be useful in the numerical analysis of geometric flows, see, e.g. [KLL19, KLL21, KLL20, BK21, BK23, BHL24, EGK22, EKL24].

The anisotropic mean curvature flow studied in this paper can be considered as the gradient flow of the anisotropic surface energy

$$\mathcal{E}_\gamma(\Gamma) = \int_\Gamma \gamma(\nu), \quad (1.1)$$

where Γ is a closed orientable C^1 -hypersurface in \mathbb{R}^{d+1} , $d \geq 1$, with a continuous unit normal field ν , and $\gamma: \mathbb{S}^d \rightarrow \mathbb{R}_{>0}$ is a given anisotropic energy density. It is helpful, to extend γ to a function on \mathbb{R}^{d+1} as a positively one-homogeneous function.

In order to visualize the surface energy, it is convenient to consider a generalized isoperimetric problem for the surface energy \mathcal{E}_γ . One wants to find the shape, which minimizes \mathcal{E}_γ under all shapes with a given enclosed volume. In order to do so, one defines the dual function

$$\gamma^*(q) = \sup_{p \in \mathbb{R}^{d+1} \setminus \{0\}} \frac{p \cdot q}{\gamma(p)} \quad \forall q \in \mathbb{R}^{d+1}.$$

Then the solution of the isoperimetric problem is, up to a scaling, the Wulff shape, see [Gur93] for details:

$$\mathcal{W} = \{q \in \mathbb{R}^{d+1} : \gamma^*(q) \leq 1\}.$$

This is the 1-ball of γ^* , and we also define the 1-ball of γ

$$\mathcal{F} = \{p \in \mathbb{R}^d : \gamma(p) \leq 1\},$$

which is called Frank diagram. We refer to Figure 2.1 for examples.

In many applications, flows are of interest that decrease the total anisotropic energy \mathcal{E}_γ . To derive such flows, we consider a family of closed, smooth and oriented hypersurfaces $(\Gamma(t))_{t \in [0, T]}$ and compute, see [Gig06, BDGP23] for a proof,

$$\frac{d}{dt} \mathcal{E}_\gamma(\Gamma(t)) = \int_{\Gamma(t)} H_\gamma V.$$

Here, V is the normal velocity of $\Gamma(t)$ and $H_\gamma = \nabla_\Gamma \cdot (\gamma'(\nu))$ is the anisotropic mean curvature. For ν we use the outward unit normal which leads to the sign convention that H_γ is positive for convex surfaces. We hence obtain that flows of the form

$$\beta(\nu)V = -H_\gamma \quad \text{on } \Gamma(t) \quad (1.2)$$

decrease the energy whenever the kinetic coefficient β is positive. It can be shown that (1.2) is the gradient flow of the anisotropic surface energy in the case that one uses a weighted L^2 -inner product, where the weight is given by β , see, e.g., [GNSW08, LSU25]. The above geometric evolution law has many applications both in mathematics as well as in physics and engineering. In materials science, surface motion is classified as geometric if the normal velocity

of the surface depends only on the position and the local shape of the surface. In particular, no long range effects play a role. In a review article, Taylor, Cahn and Handwerker [TCH92] discuss that in materials science applications many interface motion problems can be modeled as geometric and name crystal growth, certain types of phase change problems, grain growth and chemical etching as examples. Due to the fact that crystals are anisotropic these geometric evolution problems typically lead to laws which are similar as (1.2). We refer to [TCH92, Gur93, BP96, Gig06] for more details on anisotropic energies and anisotropic curvature flows in materials science and geometry.

Beside the case $\beta = 1$, the kinetic term $\beta = \frac{1}{\gamma}$ is of particular interest. As discussed in [BP96] one can consider the evolution in relative geometry, i.e., all quantities are referred to the given so-called Finsler metric given by γ representing the anisotropy. In this case, one obtains a gradient flow which is (1.2) with $\beta = \frac{1}{\gamma}$. Also for this particular choice of the kinetic coefficient one obtains that the Wulff shape is shrinking in a self-similar way, see Theorem 1.7.3 in [Gig06]. Let us mention that for curves it is known that always self-similar solutions exist, see [DGM96]. However, in the case $\beta \neq \frac{1}{\gamma}$ no explicit solution is known.

Analytically, anisotropic mean curvature flow is well studied. An important first result is due to Chen, Giga and Goto [CGG91], who showed existence and uniqueness of viscosity solutions. Almgren, Taylor and Wang [ATW93] used an implicit time discretization in the form of a minimizing movement scheme to show existence of solutions to (1.2). They also showed a short time existence result in the case that the anisotropy γ is smooth. A refined analysis of classical solutions in the curve case, including results on the long time behaviour are, due to Gage [Gag93], see also [MS01a]. By considering the evolution $V = -\gamma(\nu)H_\gamma$ in relative geometry, see the discussion above, Bellettini and Paolini [BP96] studied the evolution law using different approaches, such as the variational method of Almgren–Taylor–Wang, the Hamilton–Jacobi approach, and an approximation using an anisotropic Allen–Cahn equation. Chambolle and Novaga [CN07] gave simple proofs of convergence of the Almgren–Taylor–Wang variational approach, and Merriman–Bence–Osher algorithm relying on the theory of viscosity solutions. We refer to the recent paper [LSU25] who used a weak formulation of the anisotropic mean curvature operator in the BV-setting, which was introduced by [CNP10, GS11], to show a weak-strong uniqueness result.

The aim of this paper is to derive and analyze a finite element method for a parametric approach to solve (1.2). Using an idea originally developed in [KLL19] for the (isotropic) mean curvature flow, the scheme discretizes a system of evolution equations coupling the position vector X , the surface normal ν and the normal velocity V . These equations are anisotropic versions of identities derived by Huisken in [Hui84]. The resulting system is discretized in space with the help of the evolving surface finite element method [DE07] using continuous, piecewise polynomials of degree $k \geq 2$.

Main result: Under an appropriate smoothness assumption on the exact solution and for sufficiently small spatial grid size h it holds:

$$\begin{aligned} \max_{t \in [0, T]} \|X_h^\ell(\cdot, t) - X(\cdot, t)\|_{H^1(\Gamma^0)^{d+1}} &\leq Ch^k, \\ \max_{t \in [0, T]} \|(\nu_h^L, V_h^L)(\cdot, t) - (\nu, V)(\cdot, t)\|_{H^1(\Gamma[X(\cdot, t)])^{d+2}} &\leq Ch^k. \end{aligned}$$

In the above, $\Gamma[X(\cdot, t)]$ is the exact surface at time t , $\Gamma^0 = \Gamma[X(\cdot, 0)]$, and X_h^ℓ, ν_h^L, V_h^L are suitable lifts of the discrete solution X_h, ν_h, V_h to the exact surfaces Γ^0 and $\Gamma[X(\cdot, t)]$, respectively, see Section 4 for precise definitions and Theorem 5.1 for an exact formulation of the main result.

For *anisotropic* geometric flows numerical methods based on finite elements have started with Dziuk [Dzi99], showing semi-discrete error estimates for anisotropic curve shortening flow, and [DD02] showing fully discrete error estimates in the graph setting. For the crystalline flow of polygonal curves different methods have been developed in [RT92, GG00]. A numerical method based on a formulation which redistributes points tangentially and which uses a PDE for geometric quantities like curvature has been developed for curves in [MS01b, MS04], while a regularised fully discrete algorithm was proposed in [HV06]. Pozzi [Poz07] has shown spatial error estimates for curves in higher codimension, also see [Poz12] for some analytical results. Recently, two new schemes [DN23b, DN23a] were proposed for anisotropic curve shortening flow. A numerical method for the anisotropic mean curvature flow of a graph is proposed in [HB14]. Barrett, Garcke, and Nürnberg have developed a method with tangential redistributions for anisotropic flows in [BGN08a] for curves, in [BGN10] for anisotropic gradient flows for space curves, and in [BGN12] for anisotropic elastic curves.

The first parametric finite element-based algorithms for anisotropic mean curvature flow of *surfaces* were proposed in [Poz08] and [BGN08b]. Algorithms for anisotropic *Willmore* flow were proposed in [Poz15, BGN08b, PPR14], and for anisotropic *surface diffusion* in [Bur05, HV07, BGN08b, BL23, BL24] (the last method being structure-preserving). For numerical methods for anisotropic high-order geometric flows see, e.g., [HV05]. We refer to [DDE05] for a survey up to 2005, and a more recent one [BGN20] up to 2020.

For numerical methods based on level-sets or diffuse interfaces we refer, e.g., to [GSN99, LLRV09, OOTT11, GKS13, BGN13, SSVW21].

For *surfaces* evolving under an *anisotropic* geometric flow, up to our knowledge, there are no error estimates for parametric approaches in the literature.

The paper is structured as follows:

In the following section, we first present details on surface calculus, basic facts on anisotropy functions and on evolving hypersurfaces. The governing evolution equations are then derived in Section 3 together with weak formulations which will be the basis for the finite element method. The evolving surface finite element method is described in Section 4, the semi-discrete problem and the precise statement of the main result are stated in Section 5. In

Section 6 we prove the main result heavily relying on a matrix–vector formulation, consistency bounds and energy-type arguments. In Section 7 we introduce a regularized problem which will be helpful, in particular, in situations where the anisotropy is nearly crystalline. Section 8 presents numerical computations, beside others, rate of convergence simulations and simulations of anisotropic mean curvature flow with “crystalline-like” anisotropies are given. Finally, an appendix give proofs for important formulas from geometric analysis.

2 Preliminaries

2.1 Basic surface calculus

Let $\Gamma \subset \mathbb{R}^{d+1}$ ($d = 1, 2, 3$) be a smooth, embedded and closed hypersurface, oriented by a continuous unit normal field $\nu: \Gamma \rightarrow \mathbb{R}^{d+1}$. For a function $u: \Gamma \rightarrow \mathbb{R}$ we denote by $\nabla_\Gamma u: \Gamma \rightarrow \mathbb{R}^{d+1}$ the *tangential gradient* or *surface gradient* of u and write

$$\nabla_\Gamma u = (D_1 u, D_2 u, \dots, D_{d+1} u)^T,$$

so that we think of $\nabla_\Gamma u$ as a column vector. In the case of a vector-valued function $w = (w_1, \dots, w_{d+1})^T: \Gamma \rightarrow \mathbb{R}^{d+1}$, we let $\nabla_\Gamma w = (\nabla_\Gamma w_1, \dots, \nabla_\Gamma w_{d+1})$. Furthermore, we denote by $\nabla_\Gamma \cdot w = \text{tr}(\nabla_\Gamma w)$ the *surface divergence* of w , while we use the convention that the divergence of a matrix is computed column-wise. For a scalar function $u: \Gamma \rightarrow \mathbb{R}$ we let $\Delta_\Gamma u = \nabla_\Gamma \cdot \nabla_\Gamma u$ the *Laplace–Beltrami operator*.

The (extended) Weingarten map is defined by $A = \nabla_\Gamma \nu \in \mathbb{R}^{(d+1) \times (d+1)}$, which is a symmetric matrix, whose eigenvalues are the principal curvatures $\kappa_1, \dots, \kappa_d$, and 0 (corresponding to the eigenvector ν). The mean curvature of Γ is then given by $H = \sum_{j=1}^d \kappa_j = \text{tr}(A)$, where we note that H is positive for a sphere if the unit normal vector points outwards. See the review [DDE05], or [Eck04, Appendix A], etc. for these notions.

2.2 Anisotropy functions

Let $\gamma \in C^0(\mathbb{R}^{d+1}, \mathbb{R}_{\geq 0}) \cap C^4(\mathbb{R}^{d+1} \setminus \{0\}, \mathbb{R}_{> 0})$ be positively homogeneous of degree one, i.e.,

$$\gamma(\lambda w) = \lambda \gamma(w) \quad \text{for all } w \in \mathbb{R}^{d+1}, \lambda > 0. \quad (2.1)$$

Using (2.1) one verifies that

$$\gamma'(\lambda w) = \gamma'(w), \quad \gamma''(\lambda w) = \frac{1}{\lambda} \gamma''(w), \quad (2.2)$$

$$\gamma'(\lambda w) \cdot w = \gamma(w), \quad \gamma''(w) w = 0 \quad (2.3)$$

for any $w \in \mathbb{R}^{d+1} \setminus \{0\}$, $\lambda > 0$, where \cdot denotes the scalar product of two vectors. Furthermore, it can be shown that there exists $c_1 \geq 0$ such that

$$|\gamma''(v_1) - \gamma''(v_2)| \leq c_1 |v_1 - v_2| \quad \forall v_1, v_2 \in \mathbb{R}^{d+1}, \frac{1}{2} \leq |v_1|, |v_2| \leq 2, \quad (2.4)$$

$$|\gamma'''(v_1) - \gamma'''(v_2)| \leq c_1 |v_1 - v_2| \quad \forall v_1, v_2 \in \mathbb{R}^{d+1}, \frac{1}{2} \leq |v_1|, |v_2| \leq 2. \quad (2.5)$$

In what follows we shall assume that γ is strongly convex in the sense that there exists $c_0 > 0$ such that

$$w \cdot \gamma''(z)w \geq c_0 |w|^2 \quad \text{for all } z, w \in \mathbb{R}^{d+1}, |z| = 1, z \cdot w = 0. \quad (2.6)$$

As an immediate consequence of the above property we deduce that there exists $\delta > 0$ such that for all $\tilde{z}, z, w \in \mathbb{R}^{d+1}$ satisfying $\frac{1}{2} \leq |\tilde{z}|, |z| \leq 2, |\tilde{z} - z| < \delta$ and $z \cdot w = 0$:

$$w \cdot \gamma''(\tilde{z})w \geq \frac{c_0}{4} |w|^2. \quad (2.7)$$

Indeed, we infer with the help of (2.2), (2.6) and (2.4)

$$\begin{aligned} w \cdot \gamma''(\tilde{z})w &= w \cdot \gamma''(z)w + w \cdot (\gamma''(\tilde{z}) - \gamma''(z))w \\ &= \frac{1}{|z|} w \cdot \gamma''\left(\frac{z}{|z|}\right)w + w \cdot (\gamma''(\tilde{z}) - \gamma''(z))w \\ &\geq \frac{c_0}{2} |w|^2 - c_1 |\tilde{z} - z| |w|^2 \geq \left(\frac{c_0}{2} - c_1 \delta\right) |w|^2 = \frac{c_0}{4} |w|^2, \end{aligned}$$

provided that $\delta = \frac{c_0}{4c_1}$.

Example 2.1 (a) Any norm on \mathbb{R}^{d+1} which is smooth outside 0 is a possible anisotropy function γ suitable for this paper. In particular, one can take an ℓ^p -norm if $p \in (1, \infty)$.

(b) In many papers, see, e.g., [BGN10, BGN08b, BGN20], the anisotropy function $\gamma(w) = \sqrt{w \cdot Gw}$ with a positive definite and symmetric matrix $G \in \mathbb{R}^{(d+1) \times (d+1)}$ is considered. Its derivatives are given by

$$\gamma'(w) = \frac{1}{\gamma(w)} Gw, \quad \text{and} \quad \gamma''(w) = \frac{1}{\gamma(w)} G - \frac{1}{\gamma(w)^3} (Gw) \otimes (Gw),$$

in particular we then have $\gamma''(w)w = 0$ for any $w \in \mathbb{R}^{d+1}$.

(c) The above anisotropy only leads to ellipsoidal Wulff shapes. Therefore, often combinations of such anisotropy functions are considered. Following [BGN10, BGN08b], we now consider a larger class of surface energy densities, which are given as suitable norms of the ellipsoidal anisotropies. In particular, we choose

$$\gamma(w) = \left(\sum_{\ell=1}^L [\gamma_\ell(w)]^r \right)^{\frac{1}{r}}, \quad \gamma_\ell(w) = \sqrt{w \cdot G_\ell w}, \quad \ell = 1, \dots, L, \quad (2.8)$$

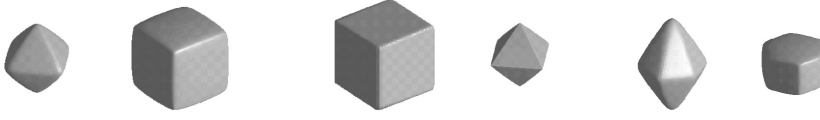


Fig. 2.1: Frank diagram and Wulff shape in \mathbb{R}^3 for a regularized ℓ^1 -norm, $\gamma(w) = \sum_{\ell=1}^3 [\varepsilon^2 |w|^2 + w_\ell^2 (1 - \varepsilon^2)]^{\frac{1}{2}}$, $\varepsilon = 0.1$, left, a cubic anisotropy, $\gamma(w) = [\sum_{\ell=1}^3 [\varepsilon^2 |w|^2 + w_\ell^2 (1 - \varepsilon^2)]^{\frac{r}{2}}]^{\frac{1}{r}}$, $\varepsilon = 0.01$, $r = 30$, middle, and a hexagonal anisotropy, $\gamma(w) = \sum_{\ell=1}^4 [w \cdot R_\ell^T \text{diag}(1, \varepsilon^2, \varepsilon^2) R_\ell w]^{\frac{1}{2}}$, $\varepsilon = 0.1$, right. Here R_ℓ , $\ell = 1, \dots, 4$ are suitable rotation matrices, see [BGN08b] for details.

so that

$$\gamma'(w) = [\gamma(w)]^{1-r} \sum_{\ell=1}^L [\gamma_\ell(w)]^{r-1} \gamma'_\ell(w).$$

Here $r \in [1, \infty)$ and $G_\ell \in \mathbb{R}^{(d+1) \times (d+1)}$, $\ell = 1, \dots, L$, are symmetric and positive definite. It turns out that most energies of relevance can be approximated by the above class of energies. In particular, hexagonal and cubic anisotropies can be modelled with appropriate choices of r , L and $\{G_\ell\}_{\ell=1}^L$, see Figure 2.1. The choice $r = 1$ has the advantage that it leads to more linear schemes. In particular, for $r = 1$ we obtain

$$\gamma''(w) = \sum_{\ell=1}^L \left[\frac{1}{\gamma_\ell(w)} G_\ell - \frac{1}{\gamma_\ell(w)^3} (G_\ell w) \otimes (G_\ell w) \right]. \quad (2.9)$$

For an oriented hypersurface Γ with unit normal ν as in Section 2.1 the vector $\gamma'(\nu)$ is called *Cahn–Hoffman vector*, while we denote by

$$H_\gamma = \nabla_\Gamma \cdot (\gamma'(\nu)) \quad (2.10)$$

the anisotropic mean curvature H_γ of Γ .

Note that in the isotropic case $\gamma(w) = |w|$ we have $\gamma'(\nu) = \nu$ so that

$$H_\gamma = \nabla_\Gamma \cdot \nu = \text{tr} \nabla_\Gamma \nu = \text{tr} A = H.$$

The following identity will be important in deriving the governing evolution equation for the surface normal ν .

Lemma 2.1 *Let $\Gamma \subset \mathbb{R}^{d+1}$ be a smooth hypersurface with unit normal ν . Then*

$$\nabla_\Gamma H_\gamma = \nabla_\Gamma \cdot (\gamma''(\nu) \nabla_\Gamma \nu) + |A|_{\gamma''}^2 \nu, \quad (2.11)$$

where we abbreviated

$$|A|_{\gamma''}^2 := |\nabla_\Gamma \nu|_{\gamma''}^2 := \nabla_\Gamma \nu : (\gamma''(\nu) \nabla_\Gamma \nu) \quad (2.12)$$

with $A : B := \text{tr}(AB^T)$ for $A, B \in \mathbb{R}^{(d+1) \times (d+1)}$.

Proof Using the definition $H_\gamma = \nabla_\Gamma \cdot (\gamma'(\nu))$ and applying the gradient–divergence interchange formula Lemma A.1 (A.4), we obtain

$$\begin{aligned} \nabla_\Gamma H_\gamma &= \nabla_\Gamma (\nabla_\Gamma \cdot (\gamma'(\nu))) \\ &= \nabla_\Gamma \cdot (\nabla_\Gamma (\gamma'(\nu)))^T + (A : \nabla_\Gamma (\gamma'(\nu)))\nu - A(\nabla_\Gamma (\gamma'(\nu)))\nu \\ &= \nabla_\Gamma \cdot (\gamma''(\nu) \nabla_\Gamma \nu) + (\nabla_\Gamma \nu : (\gamma''(\nu) \nabla_\Gamma \nu))\nu, \end{aligned}$$

where the last equality follows from

$$\nabla_\Gamma (\gamma'(\nu)) = \nabla_\Gamma \nu \gamma''(\nu) = (\gamma''(\nu) \nabla_\Gamma \nu)^T, \quad (2.13)$$

noting that both $A = \nabla_\Gamma \nu$ and $\gamma''(\nu)$ are symmetric, and by the fact that $(\nabla_\Gamma (\gamma'(\nu)))\nu = \nabla_\Gamma \nu \gamma''(\nu)\nu = 0$ in view of (2.3). Recalling (2.12) we obtain the desired form. \square

Remark 2.1 In the isotropic case $\gamma(w) = |w|$, we have $\gamma'(\nu) = \nu$, and $\gamma''(\nu) = I_{d+1} - \nu\nu^T$ so that $|A|_{\gamma''}^2 = \nabla_\Gamma \nu \cdot (\gamma''(\nu) \nabla_\Gamma \nu) = \nabla_\Gamma \nu \cdot \nabla_\Gamma \nu = |A|^2$. Hence, (2.11) reduces to the well-known identity

$$\nabla_\Gamma H = \Delta_\Gamma \nu + |A|^2 \nu. \quad (2.14)$$

2.3 Evolving hypersurfaces

Let $(\Gamma(t))_{t \in [0, T]}$ be a family of closed, smooth and oriented hypersurfaces with $G_T := \bigcup_{t \in [0, T]} (\Gamma(t) \times \{t\})$. We assume that there exists a smooth mapping $X: \Gamma^0 \times [0, T] \rightarrow \mathbb{R}^{d+1}$ such that $\Gamma(t) = \{X(p, t) : p \in \Gamma^0\}$ and that $X(\cdot, t)$ is a diffeomorphism from Γ^0 to $\Gamma(t)$. In what follows we shall abbreviate $\Gamma[X] = \Gamma[X(\cdot, t)] = \Gamma(t)$ and denote by $v: G_T \rightarrow \mathbb{R}^{d+1}$ the velocity of material points given by

$$\partial_t X(p, t) = v(X(p, t), t). \quad (2.15)$$

For a function $w: G_T \rightarrow \mathbb{R}$ we define the *material derivative* (with respect to the parametrization X) by

$$\partial^\bullet w(x, t) = \frac{d}{dt} w(X(p, t), t) \quad \text{for } x = X(p, t) \in \Gamma(t).$$

The following interchange formulas hold for sufficiently regular functions $u: G_T \rightarrow \mathbb{R}$ and vector fields $w: G_T \rightarrow \mathbb{R}^{d+1}$:

$$\partial^\bullet (\nabla_\Gamma u) = \nabla_\Gamma (\partial^\bullet u) - (\nabla_\Gamma v - \nu \nu^T (\nabla_\Gamma v)^T) \nabla_\Gamma u, \quad (2.16a)$$

$$\partial^\bullet (\nabla_\Gamma \cdot w) = \nabla_\Gamma \cdot (\partial^\bullet w) - (\nabla_\Gamma v)^T : \nabla_\Gamma w + (\nabla_\Gamma v \nu \nu^T) : \nabla_\Gamma w. \quad (2.16b)$$

See Lemma A.1 for proofs herein. We refer to [DKM13, Lemma 2.4 and 2.6] for the original componentwise formulation.

For the remainder of the paper we shall assume that the velocity vector v points in normal direction, i.e.,

$$v = V\nu,$$

where V is the normal velocity of $\Gamma(t)$.

In this setting we have the following basic identities which can be found in [Hui84, Man12, BGN20]:

$$\partial^\bullet \nu = -\nabla_\Gamma V, \quad (2.17a)$$

$$\partial^\bullet H = -\Delta_\Gamma V - |A|^2 V. \quad (2.17b)$$

In the next lemma we prove appropriate variants of (2.17) which will be useful for the anisotropic case.

Lemma 2.2 *Let $\Gamma[X]$ be a sufficiently smooth evolving hypersurface with velocity vector $v = V\nu$ and let γ be an anisotropy function. Then it holds*

$$\partial^\bullet \gamma'(\nu) = -\gamma''(\nu) \nabla_\Gamma V, \quad (2.18a)$$

$$\partial^\bullet H_\gamma = -\nabla_\Gamma \cdot \left(\gamma''(\nu) \nabla_\Gamma V \right) - |A|_{\gamma''}^2 V. \quad (2.18b)$$

Proof Equation (2.18a) follows directly from the chain rule and (2.17a), i.e.,

$$\partial^\bullet (\gamma'(\nu)) = \gamma''(\nu) \partial^\bullet \nu = -\gamma''(\nu) \nabla_\Gamma V.$$

Next, using the interchange formula (2.16b) and the definition of H_γ , we directly compute

$$\begin{aligned} \partial^\bullet H_\gamma &= \partial^\bullet (\nabla_\Gamma \cdot (\gamma'(\nu))) \\ &= \nabla_\Gamma \cdot (\partial^\bullet (\gamma'(\nu))) - (\nabla_\Gamma v)^T : \nabla_\Gamma (\gamma'(\nu)) + (\nabla_\Gamma v \nu \nu^T) : \nabla_\Gamma (\gamma'(\nu)). \end{aligned} \quad (2.19)$$

We now compute all three terms of the right-hand side more precisely.

In the first term on the right-hand side, we use (2.18a) to obtain

$$\nabla_\Gamma \cdot (\partial^\bullet (\gamma'(\nu))) = -\nabla_\Gamma \cdot \left(\gamma''(\nu) \nabla_\Gamma V \right).$$

In the second term we eliminate $v = V\nu$ and use the identity

$$\nabla_\Gamma v = \nabla_\Gamma (V\nu) = \nabla_\Gamma V \otimes \nu + V \nabla_\Gamma \nu,$$

to obtain

$$\begin{aligned} (\nabla_\Gamma v)^T : \nabla_\Gamma (\gamma'(\nu)) &= \text{tr} \left((\nabla_\Gamma V \otimes \nu + V \nabla_\Gamma \nu) \nabla_\Gamma \nu \gamma''(\nu) \right) \\ &= \text{tr} \left(\nabla_\Gamma V \nu^T \nabla_\Gamma \nu \gamma''(\nu) + V \nabla_\Gamma \nu \nabla_\Gamma \nu \gamma''(\nu) \right) \\ &= \nabla_\Gamma \nu : (\gamma''(\nu) \nabla_\Gamma \nu) V, \end{aligned}$$

where the last equality holds because both $\nabla_\Gamma \nu$ and $\gamma''(\nu)$ are symmetric and since $\nu^T \nabla_\Gamma \nu = 0$.

The third term vanishes. Indeed, by using the symmetry of $\nabla_\Gamma \nu$ and $\gamma''(\nu)$, we have

$$(\nabla_\Gamma v \nu \nu^T) : \nabla_\Gamma (\gamma'(\nu)) = \text{tr} \left(\nabla_\Gamma v \nu \nu^T \gamma''(\nu) \nabla_\Gamma \nu \right) = 0,$$

where the last equality is a consequence of (2.3). \square

3 Anisotropic mean curvature flow

3.1 Evolution law

Let γ be an anisotropy function as introduced in Section 2.2. We say that a family $(\Gamma(t))_{t \in [0, T]}$ of closed, embedded hypersurfaces evolves by anisotropic mean curvature flow if

$$\beta(\nu)V = -H_\gamma \quad \text{on } \Gamma(t). \quad (3.1)$$

Here, V is the normal velocity of $\Gamma(t)$ and $\beta \in C^2(\mathbb{R}^{d+1}, \mathbb{R}_{>0})$ is a given kinetic function. Under this assumption there exist $c_2 > 0, c_3 \geq 0$ such that

$$c_2 \leq \beta(v) \leq c_3 \quad \forall v \in \mathbb{R}^{d+1}, \frac{1}{2} \leq |v| \leq 2, \quad (3.2)$$

$$|\beta(v_1) - \beta(v_2)| \leq c_3 |v_1 - v_2| \quad \forall v_1, v_2 \in \mathbb{R}^{d+1}, \frac{1}{2} \leq |v_1|, |v_2| \leq 2, \quad (3.3)$$

$$|\beta'(v_1) - \beta'(v_2)| \leq c_3 |v_1 - v_2| \quad \forall v_1, v_2 \in \mathbb{R}^{d+1}, \frac{1}{2} \leq |v_1|, |v_2| \leq 2. \quad (3.4)$$

For the specific choice $\beta \equiv 1$ we obtain

$$V = -H_\gamma \quad \text{on } \Gamma(t). \quad (3.5)$$

In the isotropic case, (3.5) is the classical mean curvature flow, i.e., $V = -H$.

In what follows we assume a parametric description of the hypersurfaces $\Gamma(t)$ as outlined in Section 2.3, so that $\Gamma(t) = \{X(p, t) : p \in \Gamma^0\}$ for some smooth mapping $X : \Gamma^0 \times [0, T] \rightarrow \mathbb{R}^{d+1}$. Here, Γ^0 is the given initial hypersurface. In order to satisfy (3.1) taking initial conditions into account, we require

$$\partial_t X = v \circ X \quad \text{on } \Gamma^0 \times (0, T), \quad \text{where } v = V\nu, \quad (3.6a)$$

$$\beta(\nu)V = -H_\gamma = -\nabla_\Gamma \cdot (\gamma'(\nu)), \quad (3.6b)$$

$$X(\cdot, 0) = \text{id}_{\Gamma^0} \quad \text{on } \Gamma^0. \quad (3.6c)$$

In order to set up our numerical method we follow the approach introduced in [KLL19] and discretize a system that involves not only the position vector X , but also the normal vector ν and the normal velocity V . The corresponding evolution equations will be derived in the next section.

3.2 Evolution equations for anisotropic mean curvature flow

Lemma 3.1 *Let $\Gamma[X]$ be a sufficiently smooth solution of the anisotropic mean curvature flow (3.6). Then the normal vector and normal velocity satisfy*

$$\beta(\nu)\partial^\bullet \nu = \nabla_\Gamma \cdot (\gamma''(\nu)\nabla_\Gamma \nu) + |A|_{\gamma''}^2 \nu + V\nabla_\Gamma \nu \beta'(\nu), \quad (3.7a)$$

$$\beta(\nu)\partial^\bullet V = \nabla_\Gamma \cdot (\gamma''(\nu)\nabla_\Gamma V) + |A|_{\gamma''}^2 V + V\nabla_\Gamma V \cdot \beta'(\nu). \quad (3.7b)$$

Proof (a) Using (2.17a), $\beta(\nu)V = -H_\gamma$, the product rule and the chain rule yields

$$\begin{aligned}\beta(\nu)\partial^\bullet \nu &= -\beta(\nu)\nabla_\Gamma V = -\nabla_\Gamma(\beta(\nu)V) + V\nabla_\Gamma(\beta(\nu)) = \nabla_\Gamma H_\gamma + V\nabla_\Gamma \nu \beta'(\nu) \\ &= \nabla_\Gamma \cdot \left(\gamma''(\nu)\nabla_\Gamma \nu \right) + |A|_{\gamma''}^2 \nu + V\nabla_\Gamma \nu \beta'(\nu)\end{aligned}$$

in view of (2.11), which gives (3.7a).

(b) We use $\beta(\nu)V = -H_\gamma$, the product rule and the chain rule to obtain

$$\begin{aligned}\beta(\nu)\partial^\bullet V &= \partial^\bullet(\beta(\nu)V) - \partial^\bullet(\beta(\nu))V = -\partial^\bullet H_\gamma - V\beta'(\nu) \cdot \partial^\bullet \nu \\ &= \nabla_\Gamma \cdot \left(\gamma''(\nu)\nabla_\Gamma V \right) + |A|_{\gamma''}^2 V + V\nabla_\Gamma V \cdot \beta'(\nu)\end{aligned}$$

recalling (2.18b) and (2.17a). \square

Because the case $\beta \equiv 1$ is particularly relevant we state the corresponding evolution equations separately:

Corollary 3.1 *Let $\Gamma[X]$ be a sufficiently smooth solution of the anisotropic mean curvature flow (3.6) with $V = -H_\gamma$. Then the normal vector and normal velocity satisfy*

$$\partial^\bullet \nu = \nabla_\Gamma \cdot \left(\gamma''(\nu)\nabla_\Gamma \nu \right) + |A|_{\gamma''}^2 \nu, \quad (3.8a)$$

$$\partial^\bullet V = \nabla_\Gamma \cdot \left(\gamma''(\nu)\nabla_\Gamma V \right) + |A|_{\gamma''}^2 V. \quad (3.8b)$$

Remark 3.1 In the isotropic case Lemma 3.1 simplifies to the evolution equations of Huisken [Hui84]:

$$\begin{aligned}\partial^\bullet \nu &= \Delta_\Gamma \nu + |A|^2 \nu, \\ \partial^\bullet H &= \Delta_\Gamma H + |A|^2 H.\end{aligned}$$

Remark 3.2 Note that since we have $|A|_{\gamma''}^2 = \nabla_\Gamma \nu \cdot (\gamma''(\nu)\nabla_\Gamma \nu) \geq 0$, via the maximum principle for (3.8b) we conclude from $H_\gamma(\cdot, 0) \geq 0$ that $H_\gamma(\cdot, t) \geq 0$ for all $t > 0$.

3.3 Weak formulation of the coupled system

The weak formulation of the coupled system for anisotropic mean curvature flow (3.6) with (3.7) reads: Given an initial surface Γ^0 , find functions $X: \Gamma^0 \times$

$[0, T] \rightarrow \mathbb{R}^{d+1}$, $\nu: G_T \rightarrow \mathbb{R}^{d+1}$, $V: G_T \rightarrow \mathbb{R}$ such that

$$\partial_t X = v \circ X, \quad (3.9a)$$

$$v = V\nu, \quad (3.9b)$$

$$\begin{aligned} \int_{\Gamma[X]} \beta(\nu) \partial^\bullet \nu \cdot \varphi^\nu + \int_{\Gamma[X]} \gamma''(\nu) \nabla_\Gamma \nu : \nabla_\Gamma \varphi^\nu \\ = \int_{\Gamma[X]} |A|_{\gamma''}^2 \nu \cdot \varphi^\nu + \int_{\Gamma[X]} V \nabla_\Gamma \nu \beta'(\nu) \cdot \varphi^\nu, \end{aligned} \quad (3.9c)$$

$$\begin{aligned} \int_{\Gamma[X]} \beta(\nu) \partial^\bullet V \varphi^V + \int_{\Gamma[X]} \gamma''(\nu) \nabla_\Gamma V \cdot \nabla_\Gamma \varphi^V \\ = \int_{\Gamma[X]} |A|_{\gamma''}^2 V \varphi^V + \int_{\Gamma[X]} V \nabla_\Gamma V \cdot \beta'(\nu) \varphi^V, \end{aligned} \quad (3.9d)$$

for all $\varphi^\nu \in H^1(\Gamma[X])^{d+1}$ and $\varphi^V \in H^1(\Gamma[X])$. The system is endowed with geometrically compatible initial data: $X(\cdot, 0) = \text{id}_{\Gamma^0}$, $\nu(\cdot, 0) = \nu^0$ being the outward normal vector field of Γ^0 , and $V(\cdot, 0) = V^0 = -\frac{1}{\beta(\nu^0)} H_\gamma^0 = -\frac{1}{\beta(\nu^0)} \nabla_\Gamma \cdot (\gamma'(\nu^0))$.

4 Evolving surface finite element discretization

For the spatial semi-discretization of the system (3.9) we will use the evolving surface finite element method (ESFEM) [Dzi88, DE07]. We use curved simplicial finite elements and basis functions defined by continuous piecewise polynomial basis functions of degree k on triangulations, as defined in [Dem09, Section 2], [Kov18], and [ER21]. The description below is almost verbatim to [KLLP17, KLL19, EGK22].

4.1 Evolving surface finite elements

The given smooth initial surface Γ^0 is triangulated by an admissible family of triangulations \mathcal{T}_h of decreasing maximal element diameter h ; see [DE07, ER21] for the notion of an admissible triangulation, which includes quasi-uniformity and shape regularity. For a momentarily fixed h , \mathbf{x}^0 denotes the vector in $\mathbb{R}^{(d+1)N}$ that collects all nodes p_j ($j = 1, \dots, N$) of the initial triangulation. By piecewise polynomial interpolation of degree k , the nodal vector defines an approximate surface Γ_h^0 that interpolates Γ^0 in the nodes p_j . Associated with these nodes are piecewise polynomial basis function ϕ_1, \dots, ϕ_N .

Let us next fix a mapping $\mathbf{x}: [0, T] \rightarrow \mathbb{R}^{(d+1)N}$, such that $\mathbf{x}(0) = \mathbf{x}^0$. We associate with \mathbf{x} the family of discrete surfaces

$$\Gamma_h[\mathbf{x}(t)] = \Gamma[X_h(\cdot, t)] = \{X_h(p_h, t) : p_h \in \Gamma_h^0\}, \quad 0 \leq t \leq T$$

parametrized by the maps $X_h(p_h, t) = \sum_{j=1}^N x_j(t) \phi_j(p_h)$, $p_h \in \Gamma_h^0$. We abbreviate $\mathbf{x}(t)$ to \mathbf{x} when the dependence on t is clear from the context.

For $t \in [0, T]$ we introduce globally continuous finite element *basis functions* $\phi_i[\mathbf{x}(t)]: \Gamma_h[\mathbf{x}(t)] \rightarrow \mathbb{R}, i = 1, \dots, N$, such that on every element their pull-back to the reference triangle is a polynomial of degree k , which satisfies $\phi_i[\mathbf{x}(t)](x_j(t)) = \delta_{ij}$ for all $i, j = 1, \dots, N$. These functions span the finite element space

$$S_h[\mathbf{x}(t)] = S_h(\Gamma_h[\mathbf{x}(t)]) = \text{span}\{\phi_1[\mathbf{x}(t)], \phi_2[\mathbf{x}(t)], \dots, \phi_N[\mathbf{x}(t)]\}$$

and satisfy the following transport property, see [DE07],

$$\frac{d}{dt}(\phi_i[\mathbf{x}(t)](X_h(p_h, t))) = 0 \quad \forall p_h \in \Gamma_h^0. \quad (4.1)$$

For a finite element function $u_h \in S_h[\mathbf{x}(t)]$, the tangential gradient $\nabla_{\Gamma_h[\mathbf{x}(t)]} u_h$ is defined piecewise on each element. Furthermore, we define the discrete velocity $v_h(\cdot, t): \Gamma_h[\mathbf{x}(t)] \rightarrow \mathbb{R}^{d+1}$ by the relation

$$\partial_t X_h(p_h, t) = v_h(X_h(p_h, t), t).$$

In view of (4.1) we have $v_h(x, t) = \sum_{j=1}^N \dot{x}_j(t) \phi_j[\mathbf{x}(t)](x), x \in \Gamma_h[\mathbf{x}(t)]$, where the dot denotes the time derivative d/dt . In particular, the discrete velocity $v_h(\cdot, t)$ is in the finite element space $S_h[\mathbf{x}(t)]$, with nodal vector $\mathbf{v}(t) = \dot{\mathbf{x}}(t)$. Finally, the *discrete material derivative* of a finite element function $u_h(x, t)$ with nodal values $u_j(t)$ is

$$\partial_h^\bullet u_h(x, t) = \frac{d}{dt} u_h(X_h(p_h, t), t) = \sum_{j=1}^N \dot{u}_j(t) \phi_j[\mathbf{x}(t)](x) \quad \text{at } x = X_h(p_h, t).$$

Suppose that $X: \Gamma^0 \times [0, T] \rightarrow \mathbb{R}^{d+1}$ parametrizes a family of evolving surfaces $(\Gamma(t))_{t \in [0, T]}$. Defining $x^*: [0, T] \rightarrow \mathbb{R}^{(d+1)N}, x_j^*(t) := X(p_j, t)$, we then call $\Gamma_h[\mathbf{x}^*(t)] = \Gamma[X_h^*(\cdot, t)]$ the *interpolating surface* of $\Gamma(t)$. Thus, $\Gamma_h[\mathbf{x}^*(t)] = \{X_h^*(p_h, t) : p_h \in \Gamma_h^0\}$, where $X_h^*(\cdot, t) = \sum_{j=1}^N x_j^*(t) \phi_j$. In this case, the discrete velocity is given by

$$v_h^*(x, t) = \sum_{j=1}^N v_j^*(t) \phi_j[\mathbf{x}^*(t)](x) \quad \text{with } v_j^*(t) = \dot{x}_j^*(t) = \partial_t X(p_j, t). \quad (4.2)$$

Note that the evolving triangulated surface $\Gamma_h[\mathbf{x}^*(t)]$ associated with $X_h^*(\cdot, t)$ is admissible for all $t \in [0, T]$, provided that the flow map X is sufficiently regular and h is sufficiently small.

4.2 Lifts and Ritz map

Suppose again that $X: \Gamma^0 \times [0, T] \rightarrow \mathbb{R}^{d+1}$ parametrizes a family of evolving surfaces $(\Gamma(t))_{t \in [0, T]}$ with corresponding interpolating surface $\Gamma_h[\mathbf{x}^*]$. Let us denote by $d(\cdot, t)$ the oriented distance function to $\Gamma(t)$ and abbreviate $U(t) :=$

$\{x \in \mathbb{R}^{d+1} : |d(x, t)| < \delta\}$. It can be shown that for each $x \in U(t)$ there exists a unique point $x^\ell \in \Gamma[X(\cdot, t)]$ satisfying

$$x = x^\ell + d(x, t)\nu_{\Gamma[X]}(x^\ell, t) \quad (4.3)$$

provided that δ is sufficiently small. For a function $w_h : \Gamma_h[\mathbf{x}^*(t)] \rightarrow \mathbb{R}$ we define its lift $w_h^\ell : \Gamma[X(\cdot, t)] \rightarrow \mathbb{R}$ by $w_h^\ell(x^\ell) = w_h(x)$, where x and x^ℓ are connected via (4.3). It is shown in [DE13a, Lemma 4.2], that there is a constant $c > 0$ such that for all h sufficiently small and all $t \in [0, T]$ we have the bounds

$$\begin{aligned} c^{-1}\|w_h\|_{L^2(\Gamma_h[\mathbf{x}^*])} &\leq \|w_h^\ell\|_{L^2(\Gamma[X])} \leq c\|w_h\|_{L^2(\Gamma_h[\mathbf{x}^*])}, \\ c^{-1}\|w_h\|_{H^1(\Gamma_h[\mathbf{x}^*])} &\leq \|w_h^\ell\|_{H^1(\Gamma[X])} \leq c\|w_h\|_{H^1(\Gamma_h[\mathbf{x}^*])}. \end{aligned} \quad (4.4)$$

The inverse lift assigns to a function $u : \Gamma[X(\cdot, t)] \rightarrow \mathbb{R}$ the function $u^{-\ell} : \Gamma_h[\mathbf{x}^*(t)] \rightarrow \mathbb{R}$ such that $u^{-\ell}(x) = u(x^\ell)$. It is shown in [Dem09, Proposition 2.3] that

$$|\nu^{-\ell} - \nu_{\Gamma_h[\mathbf{x}^*]}| \leq ch^k, \quad (4.5)$$

where $\nu_{\Gamma_h[\mathbf{x}^*]}$ denotes the unit normal to the discrete surface $\Gamma_h[\mathbf{x}^*]$. For more details on the lift $^\ell$, see [Dzi88, DE13a, Dem09].

Let us next introduce a Ritz map, which is adjusted to our anisotropic setting. To begin, note that (2.7) together with (4.5) imply that

$$w \cdot \gamma''(\nu^{-\ell})w \geq \frac{c_0}{4}|w|^2 \quad \text{for all } w \in \mathbb{R}^{d+1}, w \cdot \nu_{\Gamma_h[\mathbf{x}^*]} = 0$$

provided that $0 < h \leq h_0$ and h_0 is small enough. This allows us to make the following definition.

Definition 4.1 Given $u \in H^1(\Gamma[X])$ we denote by $u_h^* \in S_h[\mathbf{x}^*]$ the unique solution of

$$\begin{aligned} &\int_{\Gamma_h[\mathbf{x}^*]} u_h^* \varphi_h + \int_{\Gamma_h[\mathbf{x}^*]} \gamma''(\nu^{-\ell}) \nabla_{\Gamma_h[\mathbf{x}^*]} u_h^* \cdot \nabla_{\Gamma_h[\mathbf{x}^*]} \varphi_h \\ &= \int_{\Gamma[X]} u \varphi_h^\ell + \int_{\Gamma[X]} \gamma''(\nu) \nabla_{\Gamma[X]} u \cdot \nabla_{\Gamma[X]} \varphi_h^\ell, \end{aligned} \quad (4.6)$$

for all $\varphi_h \in S_h[\mathbf{x}^*]$.

A similar Ritz map was used in [KP16, Definition 3.1], see also the variants [DE13b, Definition 6.1], [Kov18, Definition 6.1], and [ER21, Definition 3.6].

It can be shown that (cf. [KP16, Theorem 3.1–3.2] with a scalar non-linearity):

$$\|(u_h^*)^\ell - u\|_{L^2(\Gamma[X])} + h\|(u_h^*)^\ell - u\|_{H^1(\Gamma[X])} \leq Ch^{k+1}, \quad (4.7)$$

$$\|(\partial_h^\bullet u_h^*)^\ell - \partial^\bullet u\|_{L^2(\Gamma[X])} + h\|(\partial_h^\bullet u_h^*)^\ell - \partial^\bullet u\|_{H^1(\Gamma[X])} \leq Ch^{k+1}. \quad (4.8)$$

5 Discretization and main result

The evolving surface finite element spatial semi-discretization of the weak coupled parabolic system for the anisotropic mean curvature flow (3.9) reads: Find the nodal vector $\mathbf{x}(t) \in \mathbb{R}^{(d+1)N}$ and $\nu_h(\cdot, t) \in S_h[\mathbf{x}(t)]^{d+1}$, $V_h(\cdot, t) \in S_h[\mathbf{x}(t)]$ such that

$$\partial_t X_h(p_h, t) = v_h(X_h(p_h, t), t), \quad p_h \in \Gamma_h^0, \quad (5.1a)$$

$$v_h = \tilde{I}_h(V_h \nu_h), \quad (5.1b)$$

$$\begin{aligned} \int_{\Gamma_h[\mathbf{x}]} \beta(\nu_h) \partial_h^\bullet \nu_h \cdot \varphi_h^\nu + \int_{\Gamma_h[\mathbf{x}]} \gamma''(\nu_h) \nabla_{\Gamma_h[\mathbf{x}]} \nu_h : \nabla_{\Gamma_h[\mathbf{x}]} \varphi_h^\nu \\ = \int_{\Gamma_h[\mathbf{x}]} |A_h|_{\gamma_h''}^2 \nu_h \cdot \varphi_h^\nu + \int_{\Gamma_h[\mathbf{x}]} V_h \nabla_{\Gamma_h[\mathbf{x}]} \nu_h \beta'(\nu_h) \cdot \varphi_h^\nu, \end{aligned} \quad (5.1c)$$

$$\begin{aligned} \int_{\Gamma_h[\mathbf{x}]} \beta(\nu_h) \partial_h^\bullet V_h \varphi_h^V + \int_{\Gamma_h[\mathbf{x}]} \gamma''(\nu_h) \nabla_{\Gamma_h[\mathbf{x}]} V_h \cdot \nabla_{\Gamma_h[\mathbf{x}]} \varphi_h^V \\ = \int_{\Gamma_h[\mathbf{x}]} |A_h|_{\gamma_h''}^2 V_h \varphi_h^V + \int_{\Gamma_h[\mathbf{x}]} V_h \nabla_{\Gamma_h[\mathbf{x}]} V_h \cdot \beta'(\nu_h) \varphi_h^V, \end{aligned} \quad (5.1d)$$

for all $\varphi_h^V \in S_h[\mathbf{x}(t)]$ and $\varphi_h^\nu \in S_h[\mathbf{x}(t)]^{d+1}$. Here, we have abbreviated

$$A_h = \frac{1}{2} \left(\nabla_{\Gamma_h[\mathbf{x}]} \nu_h + (\nabla_{\Gamma_h[\mathbf{x}]} \nu_h)^T \right) \quad \text{and} \quad |A_h|_{\gamma_h''}^2 = A_h : \gamma''(\nu_h) A_h.$$

Furthermore, $\tilde{I}_h f := \sum_{j=1}^N f(x_j(t)) \phi_j[\mathbf{x}(t)]$ for a function $f : \Gamma_h[\mathbf{x}(t)] \rightarrow \mathbb{R}$. Finally, the initial data $\nu_h(\cdot, 0)$, and $V_h(\cdot, 0)$ are the Lagrange interpolations of ν^0 , and $V^0 = -\frac{1}{\beta(\nu^0)} H_\gamma^0 = -\frac{1}{\beta(\nu^0)} \nabla_\Gamma \cdot (\gamma'(\nu^0))$, respectively.

Our main result of this paper reads:

Theorem 5.1 *Suppose that the system (3.9) admits a sufficiently smooth, regular solution $X : \Gamma^0 \times [0, T] \rightarrow \mathbb{R}^{d+1}$ ($d = 1, 2, 3$) with unit normal ν and normal velocity V . Consider the semi-discrete problem (5.1), discretized by evolving surface finite elements of polynomial degree $k \geq 2$. Then there exists a constant $h_0 > 0$ such that for all mesh sizes $h \leq h_0$ (5.1) has a unique solution $X_h : \Gamma_h^0 \times [0, T] \rightarrow \mathbb{R}^{d+1}$, $\nu_h(\cdot, t) \in S_h[\mathbf{x}(t)]^{d+1}$, $V_h(\cdot, t) \in S_h[\mathbf{x}(t)]$ and the following error bounds hold:*

$$\begin{aligned} \max_{t \in [0, T]} \|X_h^\ell(\cdot, t) - X(\cdot, t)\|_{H^1(\Gamma^0)^{d+1}} &\leq Ch^k, \\ \max_{t \in [0, T]} \|\nu_h^L(\cdot, t) - \nu(\cdot, t)\|_{H^1(\Gamma[X(\cdot, t)])^{d+1}} &\leq Ch^k, \\ \max_{t \in [0, T]} \|V_h^L(\cdot, t) - V(\cdot, t)\|_{H^1(\Gamma[X(\cdot, t)])} &\leq Ch^k. \end{aligned}$$

Here, we have associated with a function $w_h = \sum_{j=1}^N w_j \phi_j[\mathbf{x}(t)] \in S_h[\mathbf{x}(t)]$ the function $w_h^L : \Gamma[X(\cdot, t)] \rightarrow \mathbb{R}$ via $w_h^L = (\widehat{w}_h)^\ell$, where $\widehat{w}_h = \sum_{j=1}^N w_j \phi_j[\mathbf{x}^*(t)] \in S_h[\mathbf{x}^*(t)]$, see [KLL19]. The constant C is independent of h , but depends on bounds of higher derivatives of the solution (X, ν, V) and exponentially on T .

Using the theory of analytic semigroups (see, for example, [Lun95]) it is possible to show that (1.2) possesses, locally in time, a unique smooth solution provided that γ , β and the initial data are smooth enough. For proofs of the local-in-time existence of solutions of related problems in parabolic Hölder spaces, we also refer the reader to [GG92, ATW93, MS01a], and to the discussion at the end of Chapter 1 in [Gig06].

Regularity assumptions for Theorem 5.1 are the following: We assume $X(\cdot, t) \in H^{k+1}(\Gamma^0)$, $v(\cdot, t) \in H^{k+1}(\Gamma(X(\cdot, t)))$, and for $u = (\nu, V)$ we require $u(\cdot, t), \partial^\bullet u(\cdot, t) \in W^{k+1, \infty}(\Gamma(X(\cdot, t)))^{d+2}$ with bounds that are uniform in $t \in [0, T]$.

6 Error analysis

6.1 Matrix-vector formulation

Let us write $X_h(\cdot, t) = \sum_{j=1}^N x_j(t) \phi_j$ with $\mathbf{x}(t) = (x_j(t))_{j=1}^N$ and collect the nodal values of $\nu_h(\cdot, t) \in S_h[\mathbf{x}(t)]^{d+1}$, $V_h(\cdot, t) \in S_h[\mathbf{x}(t)]$ in the column vectors $\mathbf{n} = (n_j)_{j=1}^N$, $\mathbf{V} = (V_j)_{j=1}^N$. Furthermore, we set

$$\mathbf{u} := \begin{pmatrix} \mathbf{n} \\ \mathbf{V} \end{pmatrix} \in \mathbb{R}^{(d+2)N}, \quad \text{as well as} \quad \mathbf{V} \bullet \mathbf{n} = (V_j n_j)_{j=1}^N.$$

We may then express (5.1) in matrix-vector form as

$$\dot{\mathbf{x}} = \mathbf{v}, \tag{6.1a}$$

$$\mathbf{v} = \mathbf{V} \bullet \mathbf{n}, \tag{6.1b}$$

$$\mathbf{M}^{[d+2]}(\mathbf{x}, \mathbf{u}) \dot{\mathbf{u}} + \mathbf{A}^{[d+2]}(\mathbf{x}, \mathbf{u}) \mathbf{u} = \mathbf{f}(\mathbf{x}, \mathbf{u}), \tag{6.1c}$$

where the solution-dependent mass and stiffness matrices are given by

$$\begin{aligned} \mathbf{M}(\mathbf{x}, \mathbf{u})|_{ij} &= \int_{\Gamma_h[\mathbf{x}]} \beta(\nu_h) \phi_i[\mathbf{x}] \phi_j[\mathbf{x}], \\ \mathbf{A}(\mathbf{x}, \mathbf{u})|_{ij} &= \int_{\Gamma_h[\mathbf{x}]} \gamma''(\nu_h) \nabla_{\Gamma_h} \phi_i[\mathbf{x}] \cdot \nabla_{\Gamma_h} \phi_j[\mathbf{x}] \end{aligned}$$

for $i, j = 1, \dots, N$, and we have abbreviated

$$(\mathbf{M}^{[d+2]}, \mathbf{A}^{[d+2]})(\mathbf{x}, \mathbf{u}) = I_{d+2} \otimes (\mathbf{M}, \mathbf{A})(\mathbf{x}, \mathbf{u})$$

where I_{d+2} is the identity matrix. Also $\mathbf{f}(\mathbf{x}, \mathbf{u}) = (\mathbf{f}_1(\mathbf{x}, \mathbf{u}), \mathbf{f}_2(\mathbf{x}, \mathbf{u}))^T$ with

$$\begin{aligned} \mathbf{f}_1(\mathbf{x}, \mathbf{u})|_{j+(\ell-1)N} &= \int_{\Gamma_h[\mathbf{x}]} |A_h|_{\gamma_h''}^2 \nu_{h,\ell} \phi_j[\mathbf{x}] + \int_{\Gamma_h[\mathbf{x}]} V_h (\nabla_{\Gamma_h[\mathbf{x}]} \nu_h \beta'(\nu_h))_\ell \phi_j[\mathbf{x}], \\ \mathbf{f}_2(\mathbf{x}, \mathbf{u})|_j &= \int_{\Gamma_h[\mathbf{x}]} |A_h|_{\gamma_h''}^2 V_h \phi_j[\mathbf{x}] + \int_{\Gamma_h[\mathbf{x}]} V_h \nabla_{\Gamma_h[\mathbf{x}]} V_h \cdot \beta'(\nu_h) \phi_j[\mathbf{x}], \end{aligned}$$

for $j = 1, \dots, N$ and $\ell = 1, \dots, d+1$.

Note that the above matrix–vector formulation (6.1) is particularly close to those for: mean curvature flow [KLL19, equation (3.4)] (basic structure), for generalised mean curvature flow [BK21, equation (3.4)] (solution-dependent mass matrix $\mathbf{M}(\mathbf{x}, \mathbf{u})$), and diffusion coupled to mean curvature flow [EGK22, equation (6.3)] (solution-dependent stiffness matrix $\mathbf{A}(\mathbf{x}, \mathbf{u})$). We will exploit these similarities throughout the numerical analysis of this method.

6.2 Consistency bounds

Let us define $X_h^*(\cdot, t) = \sum_{j=1}^N x_j^*(t) \phi_j$, where $x_j^*(t) = X(p_j, t)$. Furthermore, we denote by $\nu_h^* \in S_h[\mathbf{x}^*]^{d+1}$, $V_h^* \in S_h[\mathbf{x}^*]$ the Ritz maps (4.6) of ν, V , whose nodal values are collected in \mathbf{n}^* and \mathbf{V}^* respectively. As above we write

$$\mathbf{u}^* = \begin{pmatrix} \mathbf{n}^* \\ \mathbf{V}^* \end{pmatrix} \in \mathbb{R}^{(d+2)N}, \quad \text{as well as} \quad \mathbf{V}^* \bullet \mathbf{n}^* = (V_j^* n_j^*)_{j=1}^N$$

and observe that $(\mathbf{x}^*, \mathbf{n}^*, \mathbf{V}^*)$ satisfies the system

$$\dot{\mathbf{x}}^* = \mathbf{v}^*, \quad (6.2a)$$

$$\mathbf{v}^* = \mathbf{V}^* \bullet \mathbf{n}^* + \mathbf{d}_v, \quad (6.2b)$$

$$\mathbf{M}^{[d+2]}(\mathbf{x}^*, \mathbf{u}^*) \dot{\mathbf{u}}^* + \mathbf{A}^{[d+2]}(\mathbf{x}^*, \mathbf{u}^*) \mathbf{u}^* = \mathbf{f}(\mathbf{x}^*, \mathbf{u}^*) + \mathbf{M}(\mathbf{x}^*) \mathbf{d}_u. \quad (6.2c)$$

for suitably defined *defects* $d_v = \sum_{j=1}^N d_{v,j} \phi_j[\mathbf{x}^*]$, $d_u = \sum_{j=1}^N d_{u,j} \phi_j[\mathbf{x}^*]$ and with the standard mass matrix $\mathbf{M}(\mathbf{x}^*)|_{ij} = \int_{\Gamma_h[\mathbf{x}^*]} \phi_i[\mathbf{x}^*] \phi_j[\mathbf{x}^*]$.

Lemma 6.1 *We have*

$$\max_{t \in [0, T]} \|d_v(\cdot, t)\|_{H^1(\Gamma_h[\mathbf{x}^*(t)])} + \max_{t \in [0, T]} \|d_u(\cdot, t)\|_{L^2(\Gamma_h[\mathbf{x}^*(t)])} \leq Ch^k. \quad (6.3)$$

Proof Let us write $d_v = v_h^* - \tilde{I}_h^*(V_h^* \nu_h^*)$ with $v_h^* = \tilde{I}_h^*(v^{-\ell}) = \tilde{I}_h^*(V^{-\ell} \nu^{-\ell})$, where $\tilde{I}_h^* f = \sum_{j=1}^N f(x_j^*(t)) \phi_j[\mathbf{x}^*(t)]$. It is shown in [KLL21, Lemma 5.3] that

$$\|\tilde{I}_h^*(a_h b_h)\|_{H^1(\Gamma_h[\mathbf{x}^*(t)])} \leq C \|a_h\|_{H^1(\Gamma_h[\mathbf{x}^*(t)])} \|b_h\|_{W^{1,\infty}(\Gamma_h[\mathbf{x}^*(t)])}, \quad a_h, b_h \in S_h[\mathbf{x}^*(t)].$$

Combining this bound with (4.7) and the interpolation estimates from [Dem09, Proposition 2.7], and recalling (4.2), we deduce that

$$\begin{aligned} \|d_v\|_{H^1(\Gamma_h[\mathbf{x}^*(t)])} &= \|\tilde{I}_h^*(V^{-\ell} \nu^{-\ell}) - \tilde{I}_h^*(V_h^* \nu_h^*)\|_{H^1(\Gamma_h[\mathbf{x}^*(t)])} \\ &\leq \|\tilde{I}_h^*\{\tilde{I}_h^*(V^{-\ell} - V_h^*)\tilde{I}_h^* \nu^{-\ell}\}\|_{H^1(\Gamma_h[\mathbf{x}^*(t)])} \\ &\quad + \|\tilde{I}_h^*\{V_h^*(\tilde{I}_h^* \nu^{-\ell} - \nu_h^*)\}\|_{H^1(\Gamma_h[\mathbf{x}^*(t)])} \\ &\leq c \|\tilde{I}_h^*(V, \nu)^{-\ell} - (V_h^*, \nu_h^*)\|_{H^1(\Gamma_h[\mathbf{x}^*(t)])} \\ &\leq ch^k, \end{aligned}$$

where we also used that $\|\tilde{I}_h^* \nu^{-\ell}\|_{W^{1,\infty}(\Gamma_h[\mathbf{x}^*(t)])} + \|V_h^*\|_{W^{1,\infty}(\Gamma_h[\mathbf{x}^*(t)])} \leq C$.

Next, we obtain by writing (6.2c) in terms of d_u and using (3.9c), (3.9d) as well as (4.6) for $\varphi_h \in S_h[\mathbf{x}^*]^{d+2}$

$$\begin{aligned}
& \int_{\Gamma_h[\mathbf{x}^*]} d_u \cdot \varphi_h \\
&= \int_{\Gamma_h[\mathbf{x}^*]} \beta(\nu_h^*) \partial_h^\bullet u_h^* \cdot \varphi_h + \int_{\Gamma_h[\mathbf{x}^*]} \gamma''(\nu_h^*) \nabla_{\Gamma_h[\mathbf{x}^*]} u_h^* : \nabla_{\Gamma_h[\mathbf{x}^*]} \varphi_h \\
&\quad - \int_{\Gamma_h[\mathbf{x}^*]} |A_h^*|_{\gamma''}^2 u_h^* \cdot \varphi_h - \int_{\Gamma_h[\mathbf{x}^*]} V_h^* (\nabla_{\Gamma_h[\mathbf{x}^*]} u_h^*)^T \beta'(\nu_h^*) \cdot \varphi_h \\
&= \left(\int_{\Gamma_h[\mathbf{x}^*]} \beta(\nu_h^*) \partial_h^\bullet u_h^* \cdot \varphi_h - \int_{\Gamma[X]} \beta(\nu) \partial^\bullet u \cdot \varphi_h^{-\ell} \right) \\
&\quad - \left(\int_{\Gamma_h[\mathbf{x}^*]} u_h^* \cdot \varphi_h - \int_{\Gamma[X]} u \cdot \varphi_h^{-\ell} \right) \\
&\quad + \int_{\Gamma_h[\mathbf{x}^*]} (\gamma''(\nu_h^*) - \gamma''(\nu^{-\ell})) \nabla_{\Gamma_h[\mathbf{x}^*]} u_h^* : \nabla_{\Gamma_h[\mathbf{x}^*]} \varphi_h \\
&\quad - \left(\int_{\Gamma_h[\mathbf{x}^*]} |A_h^*|_{\gamma''}^2 u_h^* \cdot \varphi_h - \int_{\Gamma[X]} |A|_{\gamma''}^2 u \cdot \varphi_h^{-\ell} \right) \\
&\quad - \left(\int_{\Gamma_h[\mathbf{x}^*]} V_h^* (\nabla_{\Gamma_h[\mathbf{x}^*]} u_h^*)^T \beta'(\nu_h^*) \cdot \varphi_h - \int_{\Gamma[X]} V (\nabla_{\Gamma[X]} u)^T \beta'(\nu) \cdot \varphi_h^{-\ell} \right) \\
&=: J_1(\varphi_h) + \dots + J_5(\varphi_h).
\end{aligned}$$

By transforming the integrals over $\Gamma_h[\mathbf{x}^*]$ to $\Gamma[X]$ and using (4.7), (4.8) and (3.3) one shows that

$$|J_1(\varphi_h)| + |J_2(\varphi_h)| \leq Ch^{k+1} \|\varphi_h\|_{L^2(\Gamma_h[\mathbf{x}^*])}.$$

Next, we infer from (2.4), (4.7) and an inverse estimate that

$$\begin{aligned}
|J_3(\varphi_h)| &\leq C_1 \int_{\Gamma_h[\mathbf{x}^*]} |\nu_h^* - \nu^{-\ell}| |\nabla_{\Gamma_h[\mathbf{x}^*]} u_h^*| |\nabla_{\Gamma_h[\mathbf{x}^*]} \varphi_h| \\
&\leq C \|u_h^* - u^{-\ell}\|_{L^2(\Gamma_h[\mathbf{x}^*])} \|\nabla_{\Gamma_h[\mathbf{x}^*]} \varphi_h\|_{L^2(\Gamma_h[\mathbf{x}^*])} \\
&\leq Ch^{k+1} \|\nabla_{\Gamma_h[\mathbf{x}^*]} \varphi_h\|_{L^2(\Gamma_h[\mathbf{x}^*])} \leq Ch^k \|\varphi_h\|_{L^2(\Gamma_h[\mathbf{x}^*])}.
\end{aligned}$$

Transforming again to $\Gamma[X]$ and using (2.4), (3.4) as well as

$$| |A_h^*|_{\gamma''}^2 - |A|_{\gamma''}^2 | \leq C (|u_h^* - u^{-\ell}| + |\nabla_{\Gamma_h[\mathbf{x}^*]}(u_h^* - u^{-\ell})|)$$

we infer that

$$|J_4(\varphi_h)| + |J_5(\varphi_h)| \leq C \|u_h^* - u^{-\ell}\|_{H^1(\Gamma_h[\mathbf{x}^*])} \|\varphi_h\|_{L^2(\Gamma_h[\mathbf{x}^*])} \leq Ch^k \|\varphi_h\|_{L^2(\Gamma_h[\mathbf{x}^*])}.$$

Combining the above bounds we deduce that $|\int_{\Gamma_h[\mathbf{x}^*]} d_u \cdot \varphi_h| \leq Ch^k \|\varphi_h\|_{L^2(\Gamma_h[\mathbf{x}^*])}$ for all $\varphi_h \in S_h[\mathbf{x}^*]^{d+2}$ which yields (6.3). \square

For later use we observe that (4.7), (4.5) along with an inverse estimate imply that

$$|\nu_h^* - \nu_{\Gamma_h[\mathbf{x}^*]}| \leq |\nu_h^* - \nu^{-\ell}| + |\nu^{-\ell} - \nu_{\Gamma_h[\mathbf{x}^*]}| \leq ch^{k+1-\frac{d}{2}} + ch^k \leq \min\left(\frac{\delta}{2}, \frac{1}{4}\right) \quad (6.4)$$

if $0 < h \leq h_0$, where δ is related to (2.7). In particular, we have that

$$\frac{3}{4} \leq |\nu_h^*| \leq \frac{3}{2} \quad \text{a.e. on } \Gamma_h[\mathbf{x}^*]. \quad (6.5)$$

6.3 Auxiliary results

Let us abbreviate

$$\mathbf{e}_\mathbf{x} = \mathbf{x} - \mathbf{x}^*, \quad \mathbf{e}_\mathbf{u} = \mathbf{u} - \mathbf{u}^*, \quad \mathbf{e}_\mathbf{v} = \mathbf{v} - \mathbf{v}^* \quad (6.6)$$

with corresponding finite element functions $e_x, e_u, e_v \in S_h[\mathbf{x}^*]$. Furthermore, we shall associate with a vector $\mathbf{w} = (w_j)_{j=1}^N \in \mathbb{R}^N$ the finite element functions

$$w_h = \sum_{j=1}^N w_j \phi_j[\mathbf{x}], \quad w_h^* = \sum_{j=1}^N w_j \phi_j[\mathbf{x}^*].$$

The following norm equivalence results were shown in [KLLP17, Lemma 4.2, 4.3].

Lemma 6.2 *Suppose that $\|\nabla_{\Gamma_h[\mathbf{x}^*]} e_x\|_{L^\infty(\Gamma_h[\mathbf{x}^*])} \leq \frac{1}{4}$ and that $1 \leq p \leq \infty$. Then there exist $c_p, C_p > 0$ such that for all $\mathbf{w} \in \mathbb{R}^N$*

$$c_p \|w_h^*\|_{L^p(\Gamma_h[\mathbf{x}^*])} \leq \|w_h\|_{L^p(\Gamma_h[\mathbf{x}])} \leq C_p \|w_h^*\|_{L^p(\Gamma_h[\mathbf{x}^*])}; \quad (6.7)$$

$$c_p \|\nabla_{\Gamma_h} w_h^*\|_{L^p(\Gamma_h[\mathbf{x}^*])} \leq \|\nabla_{\Gamma_h} w_h\|_{L^p(\Gamma_h[\mathbf{x}])} \leq C_p \|\nabla_{\Gamma_h} w_h^*\|_{L^p(\Gamma_h[\mathbf{x}^*])}. \quad (6.8)$$

Lemma 6.3 *There exists $\mu > 0$ such that $\frac{1}{2} \leq |\nu_h| \leq 2$ and*

$$c \|w_h^*\|_{L^2(\Gamma_h[\mathbf{x}^*])}^2 \leq \|\mathbf{w}\|_{\mathbf{M}(\mathbf{x}, \mathbf{u})}^2 \leq C \|w_h^*\|_{L^2(\Gamma_h[\mathbf{x}^*])}^2; \quad (6.9)$$

$$c \|\nabla_{\Gamma_h} w_h^*\|_{L^2(\Gamma_h[\mathbf{x}^*])}^2 \leq \|\mathbf{w}\|_{\mathbf{A}(\mathbf{x}, \mathbf{u})}^2 \leq C \|\nabla_{\Gamma_h} w_h^*\|_{L^2(\Gamma_h[\mathbf{x}^*])}^2 \quad (6.10)$$

for all $\mathbf{w} \in \mathbb{R}^N$, provided that $\|e_u\|_{L^\infty(\Gamma_h[\mathbf{x}^*])} \leq \mu$, $\|e_x\|_{W^{1,\infty}(\Gamma_h[\mathbf{x}^*])} \leq \mu$. Here, we have abbreviated $\|\mathbf{w}\|_{\mathbf{S}}^2 = \mathbf{w}^T \mathbf{S} \mathbf{w}$ for a matrix $\mathbf{S} \in \mathbb{R}^{N \times N}$.

Proof Since $\frac{3}{4} \leq |\nu_h^*| \leq \frac{3}{2}$ there exists $\mu > 0$ such that $\frac{1}{2} \leq |\nu_h| \leq 2$ provided that $\|e_u\|_{L^\infty(\Gamma_h[\mathbf{x}^*])} \leq \mu$. Observing that $\|\mathbf{w}\|_{\mathbf{M}(\mathbf{x}, \mathbf{u})}^2 = \int_{\Gamma_h[\mathbf{x}]} \beta(\nu_h) w_h^2$, (6.9) immediately follows from (3.2) and (6.7). Next, we have in view of (6.4)

$$\begin{aligned} |\nu_h - \nu_{\Gamma_h[\mathbf{x}]}| &\leq |\nu_h - \nu_h^*| + |\nu_h^* - \nu_{\Gamma_h[\mathbf{x}^*]}| + |\nu_{\Gamma_h[\mathbf{x}^*]} - \nu_{\Gamma_h[\mathbf{x}]}| \\ &\leq \|e_u\|_{L^\infty(\Gamma_h[\mathbf{x}^*])} + \frac{\delta}{2} + c \|e_x\|_{W^{1,\infty}(\Gamma_h[\mathbf{x}^*])} < \delta, \end{aligned}$$

if $\mu > 0$ is small enough. Thus, (2.7) implies for all $v \in \mathbb{R}^{d+1}$ with $v \cdot \nu_{\Gamma_h[\mathbf{x}]} = 0$

$$v \cdot \gamma''(\nu_h)v \geq \frac{c_0}{4}|v|^2.$$

Applying this estimate with $v = \nabla_{\Gamma_h} w_h$ and observing that

$$\mathbf{w}^T \mathbf{A}(\mathbf{x}, \mathbf{u}) \mathbf{w} = \int_{\Gamma_h[\mathbf{x}]} \gamma''(\nu_h) \nabla_{\Gamma_h[\mathbf{x}]} w_h \cdot \nabla_{\Gamma_h[\mathbf{x}]} w_h,$$

we deduce the first bound in (6.10) with the help of (6.8). The second bound follows from the fact that $|\gamma''(\nu_h)| \leq \max_{\frac{1}{2} \leq |v| \leq 2} |\gamma''(v)|$. \square

Lemma 6.4 *Let $\mathbf{w}, \mathbf{z} \in \mathbb{R}^N$ and suppose that $\|z_h^*\|_{W^{1,\infty}(\Gamma_h[\mathbf{x}^*])} \leq C$. Then*

$$\mathbf{w}^T (\mathbf{M}(\mathbf{x}, \mathbf{u}) - \mathbf{M}(\mathbf{x}, \mathbf{u}^*)) \mathbf{z} \leq C \|e_u\|_{L^2(\Gamma_h[\mathbf{x}^*])} \|w_h^*\|_{L^2(\Gamma_h[\mathbf{x}^*])}; \quad (6.11)$$

$$\mathbf{w}^T (\mathbf{M}(\mathbf{x}, \mathbf{u}^*) - \mathbf{M}(\mathbf{x}^*, \mathbf{u}^*)) \mathbf{z} \leq C \|e_x\|_{H^1(\Gamma_h[\mathbf{x}^*])} \|w_h^*\|_{L^2(\Gamma_h[\mathbf{x}^*])}; \quad (6.12)$$

$$\mathbf{w}^T (\mathbf{A}(\mathbf{x}, \mathbf{u}) - \mathbf{A}(\mathbf{x}, \mathbf{u}^*)) \mathbf{z} \leq C \|e_u\|_{L^2(\Gamma_h[\mathbf{x}^*])} \|w_h^*\|_{H^1(\Gamma_h[\mathbf{x}^*])}; \quad (6.13)$$

$$\mathbf{w}^T (\mathbf{A}(\mathbf{x}, \mathbf{u}^*) - \mathbf{A}(\mathbf{x}^*, \mathbf{u}^*)) \mathbf{z} \leq C \|e_x\|_{H^1(\Gamma_h[\mathbf{x}^*])} \|w_h^*\|_{H^1(\Gamma_h[\mathbf{x}^*])}. \quad (6.14)$$

Proof The estimates (6.11), (6.13) follow from (3.3), (2.4) and Lemma 6.2 together with the fact that $|\nu_h - \nu_h^*| \leq |u_h - u_h^*|$. In order to prove the remaining bounds one can adapt Lemma 4.1 in [KLLP17] in a straightforward way and use the uniform boundedness of $\beta(\nu_h^*)$ and $\gamma''(\nu_h^*)$ respectively. \square

In order to formulate our next result we recall that the discrete velocity is given by $v_h(\cdot, t) = \sum_{j=1}^N \dot{x}_j(t) \phi_j[\mathbf{x}(t)] \in S_h[\mathbf{x}(t)]^{d+1}$.

Lemma 6.5 *Let $\mathbf{w}, \mathbf{z} \in \mathbb{R}^N$ and suppose that $\|z_h^*\|_{W^{1,\infty}(\Gamma_h[\mathbf{x}^*])} \leq C$ as well as $\|v_h\|_{W^{1,\infty}(\Gamma_h[\mathbf{x}])} \leq C$. Then*

$$\mathbf{w}^T \frac{d}{dt} \mathbf{A}(\mathbf{x}, \mathbf{u}) \mathbf{z} \leq C \|w_h^*\|_{H^1(\Gamma_h[\mathbf{x}^*])} (\|z_h^*\|_{H^1(\Gamma_h[\mathbf{x}^*])} + \|\partial_h^\bullet e_u\|_{L^2(\Gamma_h[\mathbf{x}^*])}); \quad (6.15)$$

$$\mathbf{w}^T \frac{d}{dt} (\mathbf{A}(\mathbf{x}, \mathbf{u}) - \mathbf{A}(\mathbf{x}, \mathbf{u}^*)) \mathbf{z} \leq C (\|e_u\|_{L^2(\Gamma_h[\mathbf{x}^*])} + \|\partial_h^\bullet e_u\|_{L^2(\Gamma_h[\mathbf{x}^*])}) \|w_h^*\|_{H^1(\Gamma_h[\mathbf{x}^*])}; \quad (6.16)$$

$$\mathbf{w}^T \frac{d}{dt} (\mathbf{A}(\mathbf{x}, \mathbf{u}^*) - \mathbf{A}(\mathbf{x}^*, \mathbf{u}^*)) \mathbf{z} \leq C (\|e_x\|_{H^1(\Gamma_h[\mathbf{x}^*])} + \|e_v\|_{H^1(\Gamma_h[\mathbf{x}^*])}) \|w_h^*\|_{H^1(\Gamma_h[\mathbf{x}^*])}. \quad (6.17)$$

Proof In order to prove the first bound we use Lemma 5.2 in [DE13a] with $\mathcal{A} = \gamma''(\nu_h)$ and write

$$\mathbf{w}^T \frac{d}{dt} \mathbf{A}(\mathbf{x}, \mathbf{u}) \mathbf{z} = \frac{d}{dt} \int_{\Gamma_h[\mathbf{x}]} \gamma''(\nu_h) \nabla_{\Gamma_h} w_h \cdot \nabla_{\Gamma_h} z_h = \int_{\Gamma_h[\mathbf{x}]} B(\nu_h, v_h) \nabla_{\Gamma_h} w_h \cdot \nabla_{\Gamma_h} z_h,$$

where

$$B(\nu_h, v_h) := \partial_h^\bullet \gamma''(\nu_h) + \text{tr}(\nabla_{\Gamma_h} v_h) \gamma''(\nu_h) - (\gamma''(\nu_h) \nabla_{\Gamma_h} v_h + (\gamma''(\nu_h) \nabla_{\Gamma_h} v_h)^T). \quad (6.18)$$

Since $\partial_h^\bullet \gamma''(\nu_h) = \gamma'''(\nu_h) \partial_h^\bullet \nu_h$ and $|\partial_h^\bullet \nu_h| \leq C(1 + |\partial_h^\bullet e_u|)$ we deduce (6.15) using our assumptions on $\nabla_{\Gamma_h} v_h$ and z_h^* as well as Lemma 6.2. Next, with the above relation we have

$$\mathbf{w}^T \frac{d}{dt} (\mathbf{A}(\mathbf{x}, \mathbf{u}) - \mathbf{A}(\mathbf{x}, \mathbf{u}^*)) \mathbf{z} = \int_{\Gamma_h[\mathbf{x}]} (B(\nu_h, v_h) - B(\nu_h^*, v_h)) \nabla_{\Gamma_h} w_h \cdot \nabla_{\Gamma_h} z_h.$$

Recalling (6.18) and using (2.4), (2.5) we deduce that

$$\begin{aligned} |B(\nu_h, v_h) - B(\nu_h^*, v_h)| &\leq |\gamma'''(\nu_h) \partial_h^\bullet \nu_h - \gamma'''(\nu_h^*) \partial_h^\bullet \nu_h^*| + c|\gamma''(\nu_h) - \gamma''(\nu_h^*)| \\ &\leq C(|e_u| + |\partial_h^\bullet e_u|), \end{aligned}$$

from which we infer (6.16). The remaining estimate (6.17) is obtained in a similar way as the bound (8.8) in [EGK22]. \square

6.4 Proof of the error bounds

Let us define

$$\begin{aligned} \widehat{T}_h &= \sup \left\{ t \in [0, T] : (5.1) \text{ has a solution on } [0, t], \text{ and} \right. \\ &\quad \left. \|(e_x(\cdot, s), e_v(\cdot, s), e_u(\cdot, s))\|_{W^{1,\infty}(\Gamma_h[\mathbf{x}^*(s)])} \leq h^{\frac{1}{3}}, \text{ for } 0 \leq s \leq t \right\}. \end{aligned} \quad (6.19)$$

In order to be able to apply the results of the previous section we observe that we can assume on $[0, \widehat{T}_h)$

$$\|e_x\|_{W^{1,\infty}(\Gamma_h[\mathbf{x}^*])} \leq \min\left(\frac{1}{4}, \mu\right), \quad \|e_u\|_{L^\infty(\Gamma_h[\mathbf{x}^*])} \leq \mu, \quad \|v_h\|_{W^{1,\infty}(\Gamma_h[\mathbf{x}])} \leq C,$$

provided that $0 < h \leq h_1$ and $h_1 \leq h_0$ is chosen sufficiently small. Here, the constant μ appears in Lemma 6.3. Our aim is to derive an energy type estimate for (e_x, e_v, e_u) which simultaneously proves that $\widehat{T}_h = T$ as well as the error bounds claimed in Theorem 5.1. To do so we will work with the matrix-vector form for the components of the error which we obtain from (6.1) and (6.2):

$$\dot{\mathbf{e}}_{\mathbf{x}} = \mathbf{e}_{\mathbf{v}}, \quad (6.20a)$$

$$\mathbf{e}_{\mathbf{v}} = (\mathbf{V} \bullet \mathbf{n} - \mathbf{V}^* \bullet \mathbf{n}^*) - \mathbf{d}_{\mathbf{v}}, \quad (6.20b)$$

$$\mathbf{M}(\mathbf{x}, \mathbf{u}) \dot{\mathbf{e}}_{\mathbf{u}} + \mathbf{A}(\mathbf{x}, \mathbf{u}) \mathbf{e}_{\mathbf{u}} \quad (6.20c)$$

$$\begin{aligned} &= (\mathbf{M}(\mathbf{x}^*, \mathbf{u}^*) - \mathbf{M}(\mathbf{x}, \mathbf{u})) \dot{\mathbf{u}}^* + (\mathbf{A}(\mathbf{x}^*, \mathbf{u}^*) - \mathbf{A}(\mathbf{x}, \mathbf{u})) \mathbf{u}^* \\ &\quad + (\mathbf{f}(\mathbf{x}, \mathbf{u}) - \mathbf{f}(\mathbf{x}^*, \mathbf{u}^*)) - \mathbf{M}(\mathbf{x}^*) \mathbf{d}_{\mathbf{u}}. \end{aligned}$$

Note that we have written $\mathbf{M}(\mathbf{x}, \mathbf{u})$ for $\mathbf{M}^{[d+2]}(\mathbf{x}, \mathbf{u})$, and analogously for all other matrices in order to simplify the notation. To begin, let us use the argument in [KLL21, (B), p. 628] to show that

$$\|e_v\|_{H^1(\Gamma_h[\mathbf{x}^*])} \leq C\|e_u\|_{H^1(\Gamma_h[\mathbf{x}^*])} + C\|d_v\|_{H^1(\Gamma_h[\mathbf{x}^*])}$$

and hence, recalling (6.3)

$$\|e_v(t)\|_{H^1(\Gamma_h[\mathbf{x}^*(t)])}^2 \leq Ch^{2k} + C\|e_u(t)\|_{H^1(\Gamma_h[\mathbf{x}^*(t)])}^2, \quad 0 \leq t < \widehat{T}_h. \quad (6.21)$$

Next, observing that $e_x(0) = 0$, $\partial_h^\bullet e_x = e_v$ as well as $\|\nabla_{\Gamma_h} v_h^*\|_{L^\infty(\Gamma_h[\mathbf{x}^*])} \leq C$ we may estimate with the help of (6.21)

$$\begin{aligned} & \|e_x(t)\|_{H^1(\Gamma_h[\mathbf{x}^*(t)])}^2 \\ & \leq C \int_0^t (\|e_x(s)\|_{H^1(\Gamma_h[\mathbf{x}^*(s)])} \|\partial_h^\bullet e_x(s)\|_{H^1(\Gamma_h[\mathbf{x}^*(s)])} + \|e_x(s)\|_{H^1(\Gamma_h[\mathbf{x}^*(s)])}^2) ds \\ & \leq C \int_0^t (\|e_x(s)\|_{H^1(\Gamma_h[\mathbf{x}^*(s)])}^2 + \|e_v(s)\|_{H^1(\Gamma_h[\mathbf{x}^*(s)])}^2) ds \\ & \leq Ch^{2k} + C \int_0^t (\|e_x(s)\|_{H^1(\Gamma_h[\mathbf{x}^*(s)])}^2 + \|e_u(s)\|_{H^1(\Gamma_h[\mathbf{x}^*(s)])}^2) ds. \end{aligned} \quad (6.22)$$

Similarly, using that $\|e_u(0)\|_{L^2(\Gamma_h[\mathbf{x}^*(0)])} \leq Ch^k$ we derive

$$\begin{aligned} & \|e_u(t)\|_{L^2(\Gamma_h[\mathbf{x}^*(t)])}^2 \\ & \leq Ch^{2k} + C \int_0^t (\|e_u(s)\|_{L^2(\Gamma_h[\mathbf{x}^*(s)])} \|\partial_h^\bullet e_u(s)\|_{L^2(\Gamma_h[\mathbf{x}^*(s)])} + \|e_u(s)\|_{L^2(\Gamma_h[\mathbf{x}^*(s)])}^2) ds \\ & \leq \varepsilon \int_0^t \|\partial_h^\bullet e_u(s)\|_{L^2(\Gamma_h[\mathbf{x}^*(s)])}^2 ds + Ch^{2k} + C_\varepsilon \int_0^t \|e_u(s)\|_{L^2(\Gamma_h[\mathbf{x}^*(s)])}^2 ds. \end{aligned} \quad (6.23)$$

In order to control $\nabla_{\Gamma_h} e_u$ we multiply (6.20c) by $\dot{\mathbf{e}}_u$ and deduce that

$$\begin{aligned} & \dot{\mathbf{e}}_u^T \mathbf{M}(\mathbf{x}, \mathbf{u}) \dot{\mathbf{e}}_u + \dot{\mathbf{e}}_u^T \mathbf{A}(\mathbf{x}, \mathbf{u}) \mathbf{e}_u \\ & = \dot{\mathbf{e}}_u^T (\mathbf{M}(\mathbf{x}^*, \mathbf{u}^*) - \mathbf{M}(\mathbf{x}, \mathbf{u})) \dot{\mathbf{u}}^* + \dot{\mathbf{e}}_u^T (\mathbf{A}(\mathbf{x}^*, \mathbf{u}^*) - \mathbf{A}(\mathbf{x}, \mathbf{u})) \mathbf{u}^* \\ & \quad + \dot{\mathbf{e}}_u^T (\mathbf{f}(\mathbf{x}, \mathbf{u}) - \mathbf{f}(\mathbf{x}^*, \mathbf{u}^*)) - \dot{\mathbf{e}}_u^T \mathbf{M}(\mathbf{x}^*) \mathbf{d}_u \\ & = \sum_{i=1}^4 T_i. \end{aligned} \quad (6.24)$$

The left-hand side can be estimated with the help of (6.9), (6.15) and the fact that $\|e_u\|_{W^{1,\infty}(\Gamma_h[\mathbf{x}^*])} \leq 1$:

$$\begin{aligned} & \dot{\mathbf{e}}_u^T \mathbf{M}(\mathbf{x}, \mathbf{u}) \dot{\mathbf{e}}_u + \dot{\mathbf{e}}_u^T \mathbf{A}(\mathbf{x}, \mathbf{u}) \mathbf{e}_u \\ & = \|\dot{\mathbf{e}}_u\|_{\mathbf{M}(\mathbf{x}, \mathbf{u})}^2 + \frac{1}{2} \frac{d}{dt} \|\mathbf{e}_u\|_{\mathbf{A}(\mathbf{x}, \mathbf{u})}^2 - \frac{1}{2} \mathbf{e}_u^T \frac{d}{dt} \mathbf{A}(\mathbf{x}, \mathbf{u}) \mathbf{e}_u \\ & \geq c \|\partial_h^\bullet e_u\|_{L^2(\Gamma_h[\mathbf{x}^*])}^2 + \frac{1}{2} \frac{d}{dt} \|\mathbf{e}_u\|_{\mathbf{A}(\mathbf{x}, \mathbf{u})}^2 - C \|e_u\|_{H^1(\Gamma_h[\mathbf{x}^*])} (\|e_u\|_{H^1(\Gamma_h[\mathbf{x}^*])} + \|\partial_h^\bullet e_u\|_{L^2(\Gamma_h[\mathbf{x}^*])}) \\ & \geq \frac{c}{2} \|\partial_h^\bullet e_u\|_{L^2(\Gamma_h[\mathbf{x}^*])}^2 + \frac{1}{2} \frac{d}{dt} \|\mathbf{e}_u\|_{\mathbf{A}(\mathbf{x}, \mathbf{u})}^2 - C \|e_u\|_{H^1(\Gamma_h[\mathbf{x}^*])}^2. \end{aligned} \quad (6.25)$$

Next, (6.11) and (6.12) together with the fact that $\|\partial_h^\bullet u_h^*\|_{W^{1,\infty}(\Gamma_h[\mathbf{x}^*])} \leq C$ imply that

$$\begin{aligned} T_1 & \leq C (\|e_u\|_{L^2(\Gamma_h[\mathbf{x}^*])} + \|e_x\|_{H^1(\Gamma_h[\mathbf{x}^*])}) \|\partial_h^\bullet e_u\|_{L^2(\Gamma_h[\mathbf{x}^*])} \\ & \leq \varepsilon \|\partial_h^\bullet e_u\|_{L^2(\Gamma_h[\mathbf{x}^*])}^2 + C_\varepsilon (\|e_u\|_{L^2(\Gamma_h[\mathbf{x}^*])}^2 + \|e_x\|_{H^1(\Gamma_h[\mathbf{x}^*])}^2). \end{aligned} \quad (6.26)$$

Observing that $\|\partial_h^\bullet u_h^*\|_{W^{1,\infty}(\Gamma_h[\mathbf{x}^*])} \leq C$ we infer from (6.16), (6.17), (6.13) and (6.14)

$$\begin{aligned}
T_2 &= \frac{d}{dt} (\mathbf{e}_u^T (\mathbf{A}(\mathbf{x}^*, \mathbf{u}^*) - \mathbf{A}(\mathbf{x}, \mathbf{u})) \mathbf{u}^*) - \mathbf{e}_u^T \frac{d}{dt} (\mathbf{A}(\mathbf{x}^*, \mathbf{u}^*) - \mathbf{A}(\mathbf{x}, \mathbf{u})) \mathbf{u}^* \\
&\quad - \mathbf{e}_u^T (\mathbf{A}(\mathbf{x}^*, \mathbf{u}^*) - \mathbf{A}(\mathbf{x}, \mathbf{u})) \dot{\mathbf{u}}^* \\
&\leq \frac{d}{dt} (\mathbf{e}_u^T (\mathbf{A}(\mathbf{x}^*, \mathbf{u}^*) - \mathbf{A}(\mathbf{x}, \mathbf{u})) \mathbf{u}^*) \\
&\quad + C (\|e_u\|_{L^2(\Gamma_h[\mathbf{x}^*])} + \|\partial_h^\bullet e_u\|_{L^2(\Gamma_h[\mathbf{x}^*])}) \|e_u\|_{H^1(\Gamma_h[\mathbf{x}^*])} \\
&\quad + C (\|e_x\|_{H^1(\Gamma_h[\mathbf{x}^*])} + \|e_v\|_{H^1(\Gamma_h[\mathbf{x}^*])}) \|e_u\|_{H^1(\Gamma_h[\mathbf{x}^*])} \\
&\leq \frac{d}{dt} (\mathbf{e}_u^T (\mathbf{A}(\mathbf{x}^*, \mathbf{u}^*) - \mathbf{A}(\mathbf{x}, \mathbf{u})) \mathbf{u}^*) + \varepsilon \|\partial_h^\bullet e_u\|_{L^2(\Gamma_h[\mathbf{x}^*])}^2 \\
&\quad + C_\varepsilon (h^{2k} + \|e_u\|_{H^1(\Gamma_h[\mathbf{x}^*])}^2 + \|e_x\|_{H^1(\Gamma_h[\mathbf{x}^*])}^2), \tag{6.27}
\end{aligned}$$

where we used (6.21) in the last step. Arguing as in [KLL19, (A) (vii)] one shows that

$$\begin{aligned}
T_3 &\leq C \|\partial_h^\bullet e_u\|_{L^2(\Gamma_h[\mathbf{x}^*])} (\|e_u\|_{H^1(\Gamma_h[\mathbf{x}^*])} + \|e_x\|_{H^1(\Gamma_h[\mathbf{x}^*])}) \\
&\leq \varepsilon \|\partial_h^\bullet e_u\|_{L^2(\Gamma_h[\mathbf{x}^*])}^2 + C_\varepsilon (\|e_u\|_{H^1(\Gamma_h[\mathbf{x}^*])}^2 + \|e_x\|_{H^1(\Gamma_h[\mathbf{x}^*])}^2). \tag{6.28}
\end{aligned}$$

Finally, (6.3) implies that

$$T_4 \leq \|\partial_h^\bullet e_u\|_{L^2(\Gamma_h[\mathbf{x}^*])} \|d_u\|_{L^2(\Gamma_h[\mathbf{x}^*])} \leq \varepsilon \|\partial_h^\bullet e_u\|_{L^2(\Gamma_h[\mathbf{x}^*])}^2 + C_\varepsilon h^{2k}. \tag{6.29}$$

If we insert (6.26)–(6.29) into (6.25), choose $\varepsilon > 0$ small enough we obtain after integration with respect to time and recalling that $\|e_u(0)\|_{H^1(\Gamma_h[\mathbf{x}^*(0)])} \leq Ch^k$ as well as (6.13), (6.14)

$$\begin{aligned}
&\frac{c}{4} \int_0^t \|\partial_h^\bullet e_u\|_{L^2(\Gamma_h[\mathbf{x}^*])}^2 ds + \frac{1}{2} \|\mathbf{e}_u(t)\|_{A(\mathbf{x}(t), \mathbf{u}(t))}^2 \\
&\leq Ch^{2k} + (\mathbf{e}_u(t)^T (\mathbf{A}(\mathbf{x}^*(t), \mathbf{u}^*(t)) - \mathbf{A}(\mathbf{x}(t), \mathbf{u}(t))) \mathbf{u}^*(t)) \\
&\quad + C \int_0^t (\|e_u\|_{H^1(\Gamma_h[\mathbf{x}^*])}^2 + \|e_x\|_{H^1(\Gamma_h[\mathbf{x}^*])}^2) ds \\
&\leq C \|e_u(t)\|_{H^1(\Gamma_h[\mathbf{x}^*(t)])} (\|e_u(t)\|_{L^2(\Gamma_h[\mathbf{x}^*(t)])} + \|e_x(t)\|_{H^1(\Gamma_h[\mathbf{x}^*(t)])}) \\
&\quad + Ch^{2k} + C \int_0^t (\|e_u\|_{H^1(\Gamma_h[\mathbf{x}^*])}^2 + \|e_x\|_{H^1(\Gamma_h[\mathbf{x}^*])}^2) ds \\
&\leq \varepsilon \|\nabla_{\Gamma_h} e_u(t)\|_{L^2(\Gamma_h[\mathbf{x}^*(t)])}^2 + C_\varepsilon (\|e_u(t)\|_{L^2(\Gamma_h[\mathbf{x}^*(t)])}^2 + \|e_x(t)\|_{H^1(\Gamma_h[\mathbf{x}^*(t)])}^2) \\
&\quad + Ch^{2k} + C \int_0^t (\|e_u\|_{H^1(\Gamma_h[\mathbf{x}^*])}^2 + \|e_x\|_{H^1(\Gamma_h[\mathbf{x}^*])}^2) ds.
\end{aligned}$$

If we now use (6.10) and choose $\varepsilon > 0$ small enough we infer that

$$\begin{aligned}
&\int_0^t \|\partial_h^\bullet e_u\|_{L^2(\Gamma_h[\mathbf{x}^*])}^2 ds + \|\nabla_{\Gamma_h} e_u(t)\|_{L^2(\Gamma_h[\mathbf{x}^*(t)])}^2 \\
&\leq \hat{c} (\|e_u(t)\|_{L^2(\Gamma_h[\mathbf{x}^*(t)])}^2 + \|e_x(t)\|_{H^1(\Gamma_h[\mathbf{x}^*(t)])}^2) \\
&\quad + Ch^{2k} + C \int_0^t (\|e_u\|_{H^1(\Gamma_h[\mathbf{x}^*])}^2 + \|e_x\|_{H^1(\Gamma_h[\mathbf{x}^*])}^2) ds. \tag{6.30}
\end{aligned}$$

Multiplying the inequalities (6.22), (6.23) by $\hat{c} + 1$ adding the result to (6.30) we finally obtain after choosing ε sufficiently small

$$\|(e_x, e_u)(t)\|_{H^1(\Gamma_h[\mathbf{x}^*(t)])}^2 \leq Ch^{2k} + C \int_0^t \|(e_x, e_u)(s)\|_{H^1(\Gamma_h[\mathbf{x}^*(s)])}^2 ds, \quad 0 \leq t < \hat{T}_h,$$

from which we deduce with the help of Gronwall's inequality and (6.21) that

$$\|(e_x, e_v, e_u)(t)\|_{H^1(\Gamma_h[\mathbf{x}^*(t)])} \leq Ch^k, \quad 0 \leq t < \hat{T}_h. \quad (6.31)$$

Since $k \geq 2$ and $d \in \{1, 2, 3\}$ we have that $k - \frac{d}{2} \geq \frac{1}{2}$ so that an inverse estimate implies

$$\|(e_x, e_v, e_u)(t)\|_{W^{1,\infty}(\Gamma_h[\mathbf{x}^*(t)])} \leq Ch^{k-\frac{d}{2}} \leq Ch^{\frac{1}{2}} \leq \frac{1}{2}h^{\frac{1}{3}}, \quad 0 \leq t < \hat{T}_h,$$

for $0 < h \leq h_2$ if $h_2 \leq h_1$ is small enough. Recalling (6.19) we therefore must have $\hat{T}_h = T$. In order to prove the error estimates in Theorem 5.1 we use

$$\begin{aligned} \|(\nu_h^L, V_h^L) - (\nu, V)\|_{H^1(\Gamma[X])} &= \|u_h^L - u\|_{H^1(\Gamma[X])} \\ &\leq \|u_h^L - (u_h^*)^\ell\|_{H^1(\Gamma[X])} + \|(u_h^*)^\ell - u\|_{H^1(\Gamma[X])} \\ &\leq C\|e_u\|_{H^1(\Gamma_h[\mathbf{x}^*])} + Ch^k \leq Ch^k, \end{aligned}$$

where we applied (4.7), (6.31) and the definition of u_h^L . \square

7 A stabilized algorithm

For “crystalline-like” anisotropies, e.g. those in Figure 2.1 (with small ε), the proposed algorithm greatly benefits from a stabilization of the second derivative of the anisotropy function.

In the weak formulation (3.9), let us

$$\text{replace } \gamma''(\nu) \quad \text{with} \quad \widehat{\gamma''}(\nu) := \gamma''(\nu) + \nu\nu^T. \quad (7.1)$$

It is crucial to note that $\nu\nu^T$ projects onto the normal space, hence it does not change the H^1 bilinear form and the original continuous equations (3.8) and (3.9) do not change. Naturally, since the discrete normal ν_h and the true normal of the discrete surface ν_{Γ_h} differ, this is not any more true for the semi-discretization:

$$\widehat{\gamma''}(\nu_h) = \gamma''(\nu_h) + \nu_h\nu_h^T.$$

This slight difference makes the corresponding stiffness-matrix

$$\widehat{\mathbf{A}}(\mathbf{x}, \mathbf{u}) \quad \text{more coercive.}$$

For *isotropic* mean curvature flow, $\gamma(w) = |w|$, from Remark 2.1 (cf. Example 2.1) we recall

$$\gamma''(\nu) = I_{d+1} - \nu\nu^T.$$

Using this in the discretization (5.1), the normal projection would remain. On the other hand, using the regularization would set $\widehat{\gamma}''(\nu) = \gamma''(\nu) + \nu\nu^T = I_{d+1}$. The mean curvature flow algorithm proposed in [KLL19] does not use $\gamma''(\nu_h) = I_{d+1} - \nu_h\nu_h^T$, but the identity matrix which coincides with $\widehat{\gamma}''(\nu_h) = I_{d+1}$.

It is crucial to observe that the results of Lemma 6.3–6.5 remain valid for the stabilised stiffness-matrix $\widehat{\mathbf{A}}(\mathbf{x}, \mathbf{u})$, since the used coercivity and Lipschitz properties of γ'' are, respectively, improved and unaffected (up to constants) in the case of $\widehat{\gamma}''$.

Therefore, we are confident that the statement of Theorem 5.1 holds for the stabilised algorithm as well.

8 Numerical experiments

We performed numerical simulations and experiments for the anisotropic mean curvature flow (3.6) formulated as the coupled system (3.9) in which:

- The rate of convergence in an example involving a self-similar exact solution is studied in order to illustrate the theoretical results of Theorem 5.1.
- Various anisotropic mean curvature flows with “crystalline-like”, and asymmetric anisotropies, reporting on surface evolutions and on the decreasing energy $\mathcal{E}_\gamma(\Gamma) = \int_\Gamma \gamma(\nu)$, see (1.1).
- We report on anisotropic mean curvature flows with asymmetric anisotropy, using γ from equation (8.9) in [DDE05] with $p = 4$ instead of 2.
- We report on the effects of the regularization from Section 7.

The numerical experiments use quadratic evolving surface finite elements, implemented in the Matlab package ℓ FEM [KL25]. For the computation of all finite element matrices and vectors it uses high-order quadratures so that the resulting quadrature error does not feature in the discussion of the accuracies of the schemes. The temporal discretization uses linearly-implicit BDF methods of order $1, \dots, 5$, see Section 8.1. The initial meshes were all generated using DistMesh [PS04], without taking advantage of any symmetry of the surface.

8.1 Linearly-implicit backward differentiation formulae

For the time discretization of the system of ordinary differential equations (6.1) we use a q -step linearly implicit backward difference formula (BDF method). For a step size $\tau > 0$, and with $t_n = n\tau \leq T$, we determine the approximations to all variables \mathbf{x}^n to $\mathbf{x}(t_n)$, \mathbf{v}^n to $\mathbf{v}(t_n)$, and \mathbf{u}^n to $\mathbf{u}(t_n)$, by the fully discrete system of *linear* equations, for $n \geq q$,

$$\dot{\mathbf{x}}^n = \mathbf{v}^n, \quad (8.1a)$$

$$\mathbf{v}^n = \mathbf{V}^n \bullet \mathbf{n}^n, \quad (8.1b)$$

$$\mathbf{M}^{[d+2]}(\tilde{\mathbf{x}}^n, \tilde{\mathbf{u}}^n)\dot{\mathbf{u}}^n + \mathbf{A}^{[d+2]}(\tilde{\mathbf{x}}^n, \tilde{\mathbf{u}}^n)\mathbf{u}^n = \mathbf{f}(\tilde{\mathbf{x}}^n, \tilde{\mathbf{u}}^n), \quad (8.1c)$$

where we denote the discretised time derivatives and the extrapolated values by

$$\dot{\mathbf{x}}^n = \frac{1}{\tau} \sum_{j=0}^q \delta_j \mathbf{x}^{n-j}, \quad \text{and} \quad \tilde{\mathbf{x}}^n = \sum_{j=0}^{q-1} \gamma_j \mathbf{x}^{n-1-j}, \quad n \geq q. \quad (8.2)$$

Both notations may also be used for all other variables.

The starting values \mathbf{x}^i and \mathbf{u}^i ($i = 0, \dots, q-1$) are assumed to be given. The initial values can be precomputed using either a lower order method with smaller step sizes, or an implicit Runge–Kutta method.

The method is determined by its coefficients, given by

$$\delta(\zeta) = \sum_{j=0}^q \delta_j \zeta^j = \sum_{\ell=1}^q \frac{1}{\ell} (1 - \zeta)^\ell \quad \text{and} \quad \gamma(\zeta) = \sum_{j=0}^{q-1} \gamma_j \zeta^j = (1 - (1 - \zeta)^q) / \zeta.$$

The classical BDF method is known to be zero-stable for $q \leq 6$ and to have order q ; see [HW96, Chapter V]. This order is retained, for $q \leq 5$ see [LMV13], also by the linearly-implicit variant using the above coefficients γ_j ; cf. [AL15, ALL17]. In [ACYZ20], the multiplier techniques of [NO81] have been recently extended, via a new approach, to the six-step BDF method.

8.2 Convergence test using a self-similar ellipsoid solution

Following [BGN08b, Section 5.1] we perform a numerical experiment for a self-similar ellipsoid. For $\varepsilon > 0$ we define

$$\gamma(w) = \sqrt{w \cdot G w}, \quad \text{with } G = \text{diag}(1, \varepsilon^2, \varepsilon^2), \quad \text{and} \quad \beta(w) = \frac{1}{\gamma(w)}, \quad (8.3)$$

that is the anisotropy γ from Example 2.1 (b) with a special diagonal matrix G . With this choice, one obtains

$$\gamma^*(w) = \sqrt{w \cdot G^* w}, \quad \text{with} \quad G^* = \text{diag}\left(1, \frac{1}{\varepsilon^2}, \frac{1}{\varepsilon^2}\right)$$

and as discussed in the introduction the boundary of the one ball of γ^* shrinks in a self-similar way. We hence choose the set of all points with $\gamma^*(w) = 1$ as initial surface Γ^0 , i.e., we set $\Gamma^0 := \{x \in \mathbb{R}^3 \mid d(x, 0) = 0\}$ expressed with the help of the level-set function

$$d(x, 0) = x_1^2 + x_2^2/\varepsilon^2 + x_3^2/\varepsilon^2 - 1^2.$$

The exact solution of

$$\frac{1}{\gamma(\nu)} V = -H_\gamma$$

is the hypersurface $\Gamma(t)$ which is for $t \in [0, 0.25)$ the zero level-set of the level-set function

$$d(x, t) = x_1^2 + x_2^2/\varepsilon^2 + x_3^2/\varepsilon^2 - (\sqrt{1 - 4t})^2.$$

The fact that $\Gamma(t)$ solves $\frac{1}{\gamma(\nu)}V = -H_\gamma$ can be shown as follows. Compute the outward normal field ν and normal velocity V with the help of the formulas, see, e.g., [DE07, Section 2.1] (using that $\nabla d \neq 0$),

$$\nu = \frac{\nabla d}{|\nabla d|}, \quad \text{and} \quad V = -\frac{\partial_t d}{|\nabla d|}. \quad (8.4)$$

A straightforward computation, using $\nabla_\Gamma \cdot \gamma'(\nu) = \nabla \cdot \gamma'(\nu) - \nu \cdot ((\nabla \gamma'(\nu))^T \nu)$ gives $H_\gamma = \frac{2}{\sqrt{1-4t}} = -\frac{1}{\gamma(\nu)}V$ which shows that $\Gamma(t)$ on $[0, 0.25)$ solves $\frac{1}{\gamma(\nu)}V = -H_\gamma$. Note that the surfaces $\Gamma(t)$ are identical to the sets $\sqrt{1-4t}\Gamma^0$ and satisfy $d(\cdot, t) = 0$ for all $t \in [0, 0.25]$.

We report on a convergence experiment for the above described self-similar anisotropic surface evolution with $\varepsilon = 0.5$. We started the algorithms from the nodal interpolations of the exact initial values Γ^0 , ν^0 , and $V^0 = -\beta(\nu^0)^{-1}\nabla_\Gamma \cdot (\gamma'(\nu^0))\nu^0$, subsequent initial values $i = 1, \dots, q-1$ were obtained by lower order BDF steps. In order to illustrate the convergence results of Theorem 5.1, we have computed the errors between the numerical solution (8.1) and the exact solution of (3.6). The exact nodal values of $\Gamma[X]$ were obtained by solving the ODE $\partial_t X = V\nu$, with (8.4), using, since the surface evolution is not a stiff problem, via the explicit Adams method of the same order.

The numerical solutions and energy obtained by our algorithm are plotted in Figure 8.1.

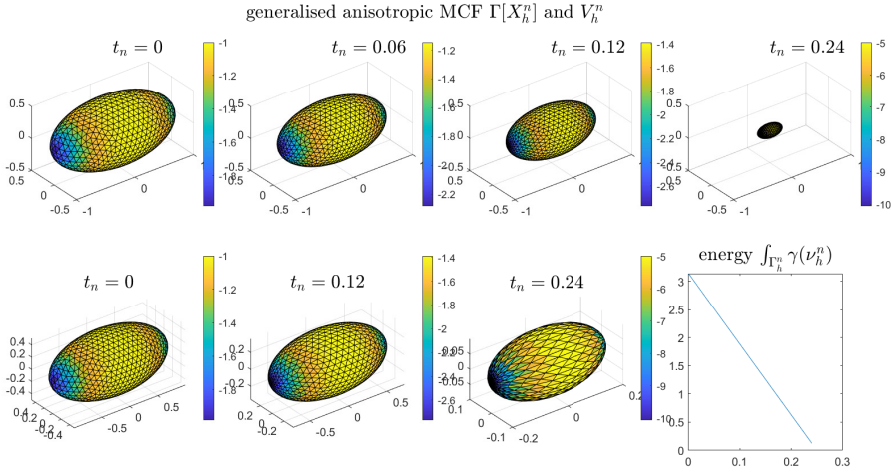


Fig. 8.1: Numerical solutions of the self-similar flow using the BDF2 / quadratic ESFEM discretization (without and with rescaling), and the decay of the anisotropic energy.

In Figure 8.2 and 8.3 we report the errors between the numerical solution and the interpolation of the exact solution until the final time $T = 0.24$, for a

sequence of meshes (see plots) and for a sequence of time steps $\tau_{k+1} = \tau_k/2$. The double-logarithmic plots report on the $L^\infty(H^1)$ norm of the errors against the mesh width h in Figure 8.2, and against the time step size τ in Figure 8.3. The lines marked with different symbols and different colours correspond to different time step sizes and to different mesh refinements in Figure 8.2 and 8.3, respectively.

In Figure 8.2 we can observe two regions: a region where the spatial discretization error dominates, matching the $\mathcal{O}(h^2)$ order of convergence of Theorem 5.1 (see the reference lines), and a region, with small mesh size, where the temporal discretization error dominates (the error curves flatten out). For Figure 8.3, the same description applies, but with reversed roles. Convergence of fully discrete method is not shown, but $\mathcal{O}(\tau^q)$ is expected for the BDF methods of order $q = 1, \dots, 5$, cf. [KLL19].

The spatial convergence as shown by Figure 8.2 is in agreement with the theoretical convergence results (note the reference lines). Similarly, the temporal convergence as shown by Figure 8.3 is in agreement with the *expected* convergence rate of the BDF2 method, cf. [KLL19].

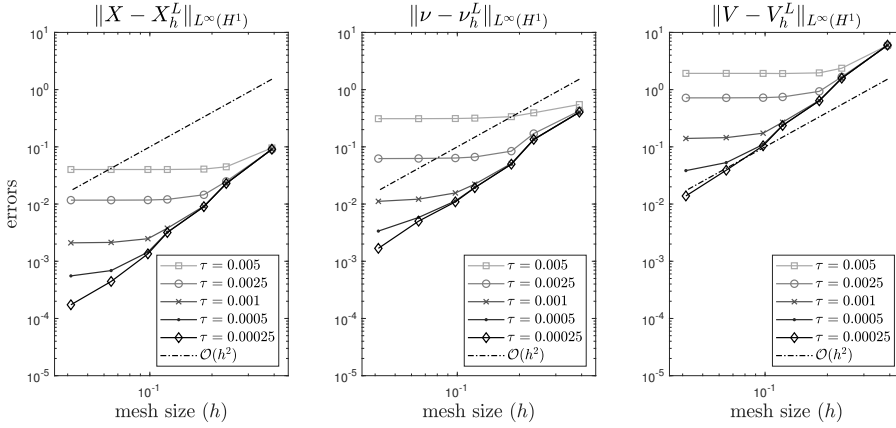


Fig. 8.2: Spatial convergence of the BDF2 / quadratic ESFEM discretization of the anisotropic flow for the self-similar ellipsoid with $T = 0.24$.

Most closed surfaces shrink to a Wulff-shaped point in finite time under anisotropic mean curvature flow (3.6), similarly as (uniformly convex) closed surfaces shrink to a round point in finite time under mean curvature flow, [Hui84, Theorem 1.1].

Figure 8.4 reports on the evolution of a spherical initial surface under anisotropic mean curvature flow setting (8.3) with $\varepsilon = 0.1$.

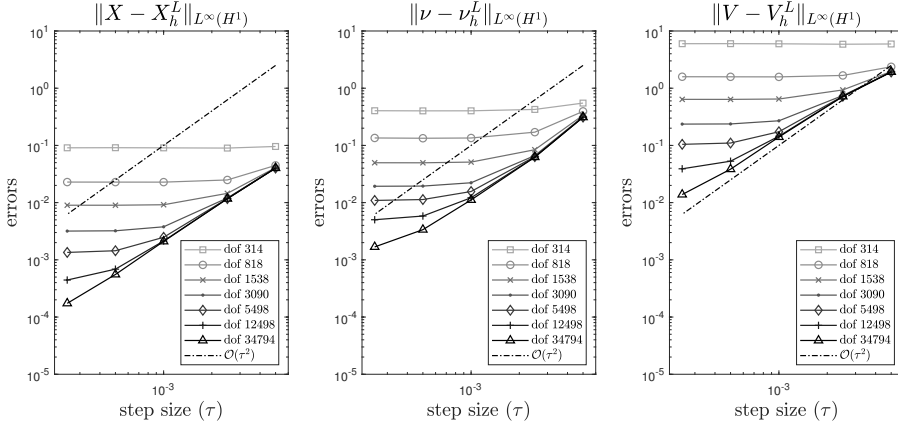


Fig. 8.3: Temporal convergence of the BDF2 / quadratic ESFEM discretization of the anisotropic flow for the self-similar ellipsoid with $T = 0.24$.

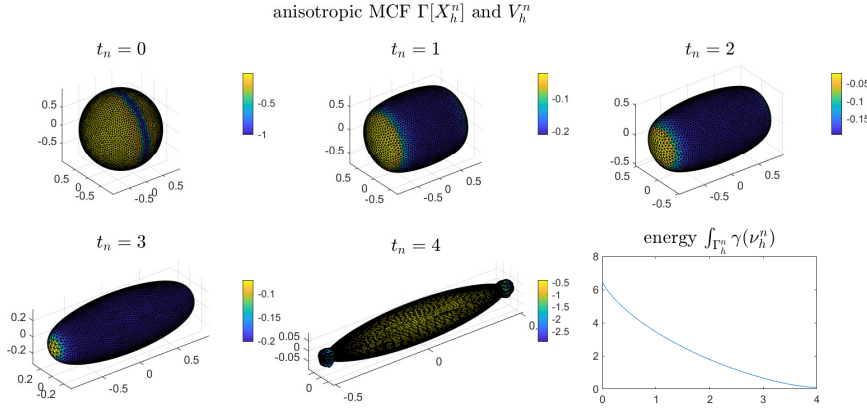


Fig. 8.4: Numerical solutions of the ellipsoidal anisotropic MCF using the BDF2 / quadratic ESFEM discretization ($\varepsilon = 0.1$, dof = 3882, and $\tau = 10^{-3}$), and the decay of the anisotropic energy.

8.3 Crystalline-like anisotropies

We have performed some numerical experiments with two “*crystalline-like*” anisotropies from [BGN08b]. In particular we use the cubic and hexagonal anisotropy function (regularized with $\varepsilon = 0.1$) described in Example 2.1 (c), and see Figure 2.1 depicting the corresponding Wulff shapes and [BGN08b, page 9] for precise definitions.

Note that both these anisotropies are quite irregular (the Wulff shapes having ε -regularized edges), whereas our numerical algorithm is particularly suitable for regular anisotropies, see Figure 8.4 with γ from (8.3) with $\varepsilon = 0.1$

and $\beta \equiv 1$. Nevertheless, the algorithm performs quite well, see Figure 8.5 and 8.6.

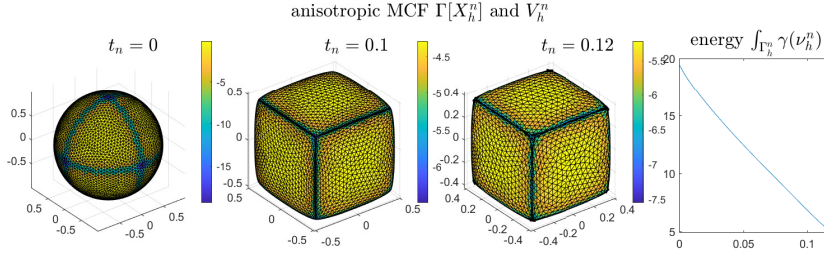


Fig. 8.5: Numerical solutions of the cubic ($\varepsilon = 0.1$) anisotropic MCF using the BDF2 / quadratic ESFEM discretization (dof = 3882 and $\tau = 10^{-3}$), and the decay of the anisotropic energy.

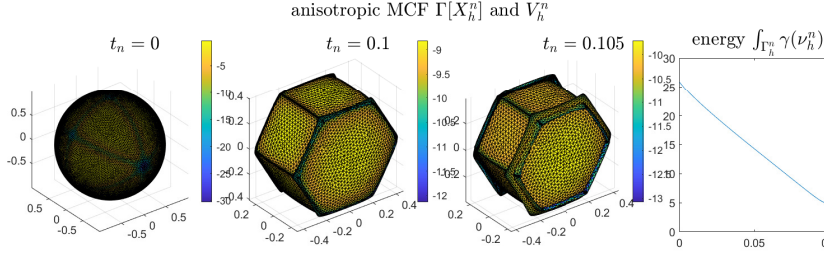


Fig. 8.6: Numerical solutions of the hexagonal ($\varepsilon = 0.1$) anisotropic MCF using the BDF2 / quadratic ESFEM discretization (dof = 12066 and $\tau = 10^{-3}$), and the decay of the anisotropic energy.

8.4 Asymmetric anisotropy

We have performed numerical experiments for anisotropic mean curvature flow (3.6) with *asymmetric* anisotropy

$$\gamma(w) = \left((5.5 + 4.5 \operatorname{sign}(w_1)) w_1^p + w_2^p + w_3^p \right)^{1/p}, \quad \text{with } p := 4, \quad (8.5)$$

from equation (8.9) in [DDE05] with exponent $p = 4$ instead of 2. See [DDE05, Figure 8.2] for Frank diagram and Wulff shape with $p = 2$.

In the spirit of Example 2.1 (b): Setting $a(w_1) = 5.5 + 4.5 \operatorname{sign}(w_1)$ and

$$G(w_1) := \operatorname{diag}(a(w_1), 1, 1) \in \mathbb{R}^{3 \times 3},$$

and therefore rewriting

$$\gamma(w) = \left(w \cdot G(w_1) w^{p-1} \right)^{1/p},$$

where $w^q|_j = w_j^q$ for all $j = 1, 2, 3$ and any q .

We further keep $p \geq 4$ general, and note that (for such p) $(\text{sign}(x)x^p)' = (|x|x^{p-1})' = p|x|x^{p-2} = p \text{sign}(x)x^{p-1}$ and $(|x|x^{p-1})'' = p(p-1)|x|x^{p-3} = p(p-1) \text{sign}(x)x^{p-2}$.

The derivative of γ is then given by

$$\gamma'(w) = (\gamma(w))^{1-p} G(w_1) w^{p-1},$$

while second derivative is given by

$$\begin{aligned} \gamma''(w) &= (p-1)(\gamma(w))^{1-p} \text{diag}(G(w_1)w^{p-2}) \\ &\quad + (1-p)(\gamma(w))^{1-2p} (G(w_1)w^{p-1}) \otimes (G(w_1)w^{p-1}), \end{aligned}$$

cf. the derivatives in Example 2.1 (b).

Using the anisotropy (8.5) (and $\beta \equiv 1$), the surface evolution and the decay of the anisotropic energy are reported in Figure 8.7.

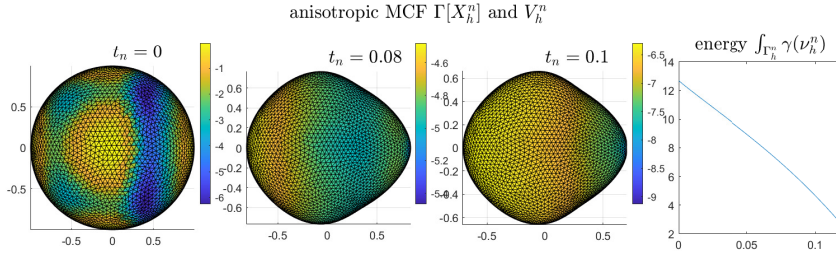


Fig. 8.7: Numerical solutions of the anisotropic MCF with the asymmetric function (8.5) using the BDF2 / quadratic ESFEM discretization (dof = 3882 and $\tau = 10^{-3}$), and the decay of the anisotropic energy.

8.5 Experiments with the stabilized algorithm

We have performed some numerical experiments using the stabilization of Section 7:

$$\widehat{\gamma}''(\nu) := \gamma''(\nu) + \nu\nu^T.$$

In Figure 8.8 we compare the numerical solutions without and with the above stabilization.

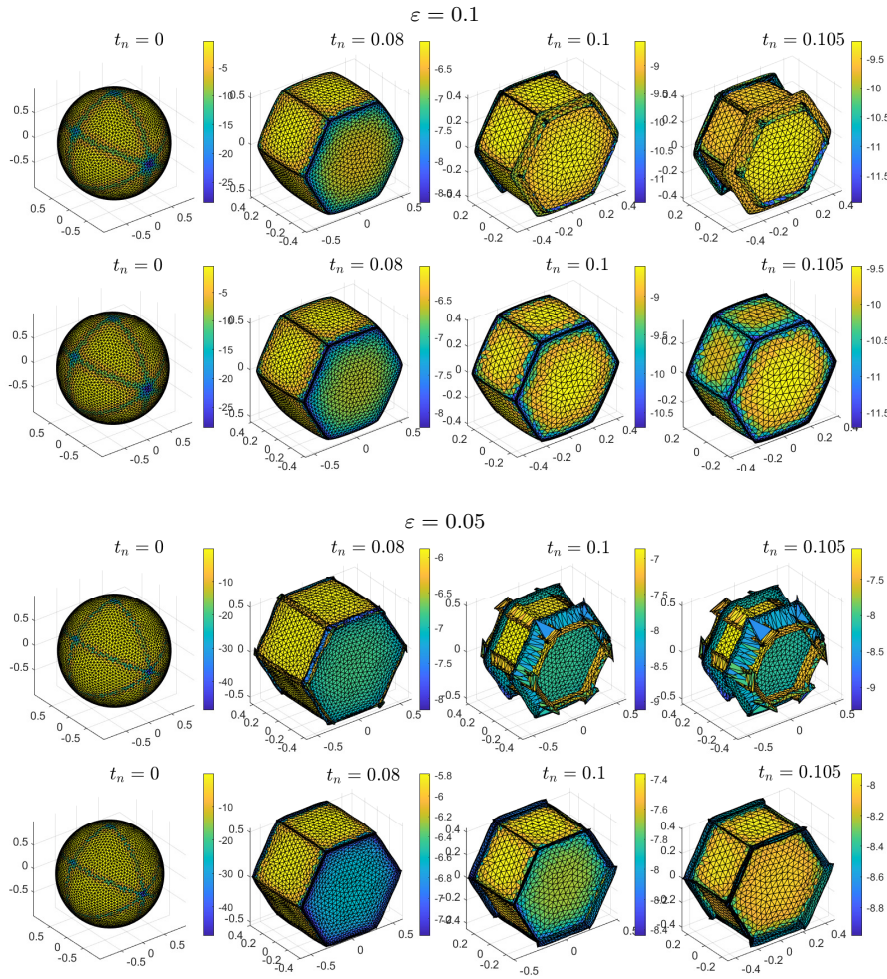


Fig. 8.8: Stabilization effect: comparing numerical solutions of with hexagonal anisotropy ($\varepsilon = 0.1$ and $\varepsilon = 0.05$) odd rows without, and even rows with stabilization.

Acknowledgments

The work of Harald Garcke is supported by the DFG Research Training Group 2339 *IntComSin* – Project-ID 321821685.

The work of Balázs Kovács is funded by the Heisenberg Programme of the Deutsche Forschungsgemeinschaft (DFG, German Research Foundation) – Project-ID 446431602, and by the DFG Research Unit FOR 3013 *Vector- and tensor-valued surface PDEs* (BA2268/6–1).

A Proofs of interchange formulas

The following interchange formulas for coordinate-wise differential operators were proved in [DKM13, Lemma 2.4 and 2.6]:

$$D_i D_k u = D_k D_i u + A_{kl} D_l u \nu_i - A_{il} D_l u \nu_k, \quad (\text{A.1a})$$

$$\partial^\bullet(D_i u) = D_i(\partial^\bullet u) - (D_i v_j - \nu_k \nu_i D_j v_k) D_j u. \quad (\text{A.1b})$$

The following lemma translates these to surface gradient and surface divergence operators. We remind that we use the convention that the divergence of a matrix is computed column-wise.

Lemma A.1 (interchange formulas) *Let $u: \Gamma(t) \rightarrow \mathbb{R}$ and $w: \Gamma(t) \rightarrow \mathbb{R}^{d+1}$ be C^2 functions on a C^2 surface $\Gamma(t)$ evolving with velocity v . Then the following identities hold*

$$\nabla_\Gamma^2 u = (\nabla_\Gamma^2 u)^T + \nu \otimes (A \nabla_\Gamma u) - (A \nabla_\Gamma u) \otimes \nu, \quad (\text{A.2})$$

$$\partial^\bullet(\nabla_\Gamma u) = \nabla_\Gamma(\partial^\bullet u) - (\nabla_\Gamma v - \nu \nu^T (\nabla_\Gamma v)^T) \nabla_\Gamma u, \quad (\text{A.3})$$

$$\nabla_\Gamma(\nabla_\Gamma \cdot w) = \Delta_\Gamma w + (A : \nabla_\Gamma w) \nu - A(\nabla_\Gamma w \nu), \quad (\text{A.4})$$

$$\partial^\bullet(\nabla_\Gamma \cdot w) = \nabla_\Gamma \cdot (\partial^\bullet w) - (\nabla_\Gamma v)^T : \nabla_\Gamma w + (\nabla_\Gamma v \nu \nu^T) : \nabla_\Gamma w. \quad (\text{A.5})$$

Proof (i) The first identity follows directly from (A.1a).

(ii) The second identity follows from (A.1b).

(iii) For the third identity we use (A.1a) and the fact that $A = \nabla_\Gamma \nu$ is a symmetric matrix, combining these gives

$$\begin{aligned} \nabla_\Gamma(\nabla_\Gamma \cdot w) &= D_i D_k w_k \\ &= D_k D_i w_k + A_{kj} D_j w_k \nu_i - A_{ij} D_j w_k \nu_k \\ &= D_k D_i w_k + A_{jk} D_j w_k \nu_i - A_{ji} D_j w_k \nu_k \\ &= \nabla_\Gamma \cdot (\nabla_\Gamma w)^T + (A : \nabla_\Gamma w) \nu - A(\nabla_\Gamma w \nu). \end{aligned}$$

(iv) For the fourth identity we again use (A.1b) and the definition of surface divergence, which together give

$$\begin{aligned} \partial^\bullet(\nabla_\Gamma \cdot w) &= \partial^\bullet(D_i w_i) \\ &= D_i(\partial^\bullet w_i) - (D_i v_j - \nu_k \nu_i D_j v_k) D_j w_i \\ &= \nabla_\Gamma \cdot (\partial^\bullet w) - ((\nabla_\Gamma v)^T - \nabla_\Gamma v \nu \nu^T) : \nabla_\Gamma w. \end{aligned}$$

□

References

- ACYZ20. G. Akrivis, M. Chen, F. Yu, and Z. Zhou. The energy technique for the six-step BDF method. *arXiv:2007.08924*, 2020.
- AL15. G. Akrivis and Ch. Lubich. Fully implicit, linearly implicit and implicit–explicit backward difference formulae for quasi-linear parabolic equations. *Numer. Math.*, 131(4):713–735, 2015.
- ALL17. G. Akrivis, B. Li, and Ch. Lubich. Combining maximal regularity and energy estimates for time discretizations of quasilinear parabolic equations. *Math. Comp.*, 86(306):1527–1552, 2017.
- ATW93. F. Almgren, J. E. Taylor, and L. Wang. Curvature-driven flows: a variational approach. *SIAM J. Control Optim.*, 31(2):387–438, 1993.
- BDGP23. E. Bänsch, K. Deckelnick, H. Garcke, and P. Pozzi. *Interfaces: modeling, analysis, numerics*, volume 51 of *Oberwolfach Seminars*. Birkhäuser/Springer, Cham, 2023.
- BGN08a. J. W. Barrett, H. Garcke, and R. Nürnberg. Numerical approximation of anisotropic geometric evolution equations in the plane. *IMA J. Numer. Anal.*, 28(2):292–330, 2008.
- BGN08b. J. W. Barrett, H. Garcke, and R. Nürnberg. A variational formulation of anisotropic geometric evolution equations in higher dimensions. *Numer. Math.*, 109(1):1–44, 2008.
- BGN10. J. W. Barrett, H. Garcke, and R. Nürnberg. Numerical approximation of gradient flows for closed curves in \mathbb{R}^d . *IMA J. Numer. Anal.*, 30(1):4–60, 2010.
- BGN12. J. W. Barrett, H. Garcke, and R. Nürnberg. Parametric approximation of isotropic and anisotropic elastic flow for closed and open curves. *Numer. Math.*, 120(3):489–542, 2012.
- BGN13. J. W. Barrett, Harald Garcke, and Robert Nürnberg. On the stable discretization of strongly anisotropic phase field models with applications to crystal growth. *ZAMM Z. Angew. Math. Mech.*, 93(10-11):719–732, 2013.
- BGN20. J. W. Barrett, H. Garcke, and R. Nürnberg. Parametric finite element approximations of curvature driven interface evolutions. In Andrea Bonito and Riccardo H. Nochetto, editors, *Handb. Numer. Anal.*, volume 21, pages 275–423. Elsevier, Amsterdam, 2020.
- BHL24. G. Bai, J. Hu, and B. Li. A convergent evolving finite element method with artificial tangential motion for surface evolution under a prescribed velocity field. *SIAM J. Numer. Anal.*, 62(5):2172–2195, 2024.
- BK21. T. Binz and B. Kovács. A convergent finite element algorithm for generalized mean curvature flows of closed surfaces. *IMA J. Numer. Anal.*, 2021. doi:10.1093/imanum/drab043.
- BK23. T. Binz and B. Kovács. A convergent finite element algorithm for mean curvature flow in arbitrary codimension. *Interfaces Free Bound.*, 25(3):373–400, 2023.
- BL23. W. Bao and Y. Li. A symmetrized parametric finite element method for anisotropic surface diffusion in three dimensions. *SIAM J. Sci. Comput.*, 45(4):A1438–A1461, 2023.
- BL24. W. Bao and Y. Li. A structure-preserving parametric finite element method for geometric flows with anisotropic surface energy. *Numer. Math.*, 156(2):609–639, 2024.
- BP96. G. Bellettini and M. Paolini. Anisotropic motion by mean curvature in the context of Finsler geometry. *Hokkaido Math. J.*, 25(3):537–566, 1996.
- Bur05. M. Burger. Numerical simulation of anisotropic surface diffusion with curvature-dependent energy. *J. Comput. Phys.*, 203(2):602–625, 2005.
- CGG91. Y. G. Chen, Y. Giga, and S. Goto. Uniqueness and existence of viscosity solutions of generalized mean curvature flow equations. *J. Differential Geom.*, 33(3):749–786, 1991.
- CN07. A. Chambolle and M. Novaga. Approximation of the anisotropic mean curvature flow. *Math. Models Methods Appl. Sci.*, 17(6):833–844, 2007.
- CNP10. M. Cicalese, Y. Nagase, and G. Pisante. The Gibbs-Thomson relation for non homogeneous anisotropic phase transitions. *Adv. Calc. Var.*, 3(3):321–344, 2010.

- DD02. K. Deckelnick and G. Dziuk. A fully discrete numerical scheme for weighted mean curvature flow. *Numer. Math.*, 91(3):423–452, 2002.
- DDE05. K. Deckelnick, G. Dziuk, and C. M. Elliott. Computation of geometric partial differential equations and mean curvature flow. *Acta Numerica*, 14:139–232, 2005.
- DE07. G. Dziuk and C. M. Elliott. Finite elements on evolving surfaces. *IMA J. Numer. Anal.*, 27(2):262–292, 2007.
- DE13a. G. Dziuk and C. M. Elliott. Finite element methods for surface PDEs. *Acta Numerica*, 22:289–396, 2013.
- DE13b. G. Dziuk and C. M. Elliott. L^2 -estimates for the evolving surface finite element method. *Math. Comp.*, 82(281):1–24, 2013.
- Dem09. A. Demlow. Higher-order finite element methods and pointwise error estimates for elliptic problems on surfaces. *SIAM J. Numer. Anal.*, 47(2):805–807, 2009.
- DGM96. C. Dohmen, Y. Giga, and N. Mizoguchi. Existence of selfsimilar shrinking curves for anisotropic curvature flow equations. *Calc. Var. Partial Differential Equations*, 4(2):103–119, 1996.
- DKM13. G. Dziuk, D. Kröner, and T. Müller. Scalar conservation laws on moving hypersurfaces. *Interfaces Free Bound.*, 15(2):203–236, 2013.
- DN23a. K. Deckelnick and R. Nürnberg. A novel finite element approximation of anisotropic curve shortening flow. *Interfaces Free Bound.*, 25(4):671–708, 2023.
- DN23b. K. Deckelnick and R. Nürnberg. An unconditionally stable finite element scheme for anisotropic curve shortening flow. *Arch. Math. (Brno)*, 59(3):263–274, 2023.
- Dzi88. G. Dziuk. Finite elements for the Beltrami operator on arbitrary surfaces. *Partial differential equations and calculus of variations, Lecture Notes in Math.*, 1357, Springer, Berlin, pages 142–155, 1988.
- Dzi99. G. Dziuk. Discrete anisotropic curve shortening flow. *SIAM J. Numer. Anal.*, 36(6):1808–1830, 1999.
- Eck04. K. Ecker. *Regularity theory for mean curvature flow*, volume 57 of *Progress in Nonlinear Differential Equations and their Applications*. Birkhäuser Boston, Boston, MA, 2004.
- EGK22. C. M. Elliott, H. Garcke, and B. Kovács. Numerical analysis for the interaction of mean curvature flow and diffusion on closed surfaces. *Numer. Math.*, 151(4):873–925, 2022.
- EKL24. D. Edelmann, B. Kovács, and Ch. Lubich. Numerical analysis of an evolving bulk-surface model of tumour growth. *IMA Journal of Numerical Analysis*, 2024.
- ER21. C. M. Elliott and T. Ranner. A unified theory for continuous-in-time evolving finite element space approximations to partial differential equations in evolving domains. *IMA Journal of Numerical Analysis*, 41:1696–1845, 2021.
- Gag93. M. E. Gage. Evolving plane curves by curvature in relative geometries. *Duke Math. J.*, 72(2):441–466, 1993.
- GG92. Y. Giga and S. Goto. Geometric evolution of phase-boundaries. In *On the evolution of phase boundaries (Minneapolis, MN, 1990–91)*, volume 43 of *IMA Vol. Math. Appl.*, pages 51–65. Springer, New York, 1992.
- GG00. M.-H. Giga and Y. Giga. Crystalline and level set flow—convergence of a crystalline algorithm for a general anisotropic curvature flow in the plane. In *Free boundary problems: theory and applications, I (Chiba, 1999)*, volume 13 of *GAKUTO Internat. Ser. Math. Sci. Appl.*, pages 64–79. Gakkotosho, Tokyo, 2000.
- Gig06. Y. Giga. *Surface evolution equations*, volume 99 of *Monographs in Mathematics*. Birkhäuser Verlag, Basel, 2006.
- GKS13. C. Gräser, R. Kornhuber, and U. Sack. Time discretizations of anisotropic Allen-Cahn equations. *IMA J. Numer. Anal.*, 33(4):1226–1244, 2013.
- GNSW08. H. Garcke, B. Nestler, B. Stinner, and F. Wendler. Allen-Cahn systems with volume constraints. *Math. Models Methods Appl. Sci.*, 18(8):1347–1381, 2008.
- GS11. H. Garcke and S. Schaubeck. Existence of weak solutions for the Stefan problem with anisotropic Gibbs-Thomson law. *Adv. Math. Sci. Appl.*, 21(1):255–283, 2011.

- GSN99. H. Garcke, B. Stoth, and B. Nestler. Anisotropy in multi-phase systems: a phase field approach. *Interfaces Free Bound.*, 1(2):175–198, 1999.
- Gur93. M. E. Gurtin. *Thermomechanics of evolving phase boundaries in the plane*. Oxford Mathematical Monographs. The Clarendon Press, Oxford University Press, New York, 1993.
- HB14. D. H. Hoang and M. Beneš. Forced anisotropic mean curvature flow of graphs in relative geometry. *Math. Bohem.*, 139(2):429–436, 2014.
- Hui84. G. Huisken. Flow by mean curvature of convex surfaces into spheres. *J. Differential Geometry*, 20(1):237–266, 1984.
- HV05. F. Hauser and A. Voigt. A discrete scheme for regularized anisotropic surface diffusion: a 6th order geometric evolution equation. *Interfaces Free Bound.*, 7(4):353–369, 2005.
- HV06. F. Hauser and A. Voigt. A numerical scheme for regularized anisotropic curve shortening flow. *Appl. Math. Lett.*, 19(8):691–698, 2006.
- HV07. F. Hauser and A. Voigt. A discrete scheme for parametric anisotropic surface diffusion. *J. Sci. Comput.*, 30(2):223–235, 2007.
- HW96. E. Hairer and G. Wanner. *Solving Ordinary Differential Equations II. Stiff and Differential-Algebraic Problems*. Springer, Berlin, Second edition, 1996.
- KL25. B. Kovács and M. F. R. Lantelme. ℓ FEM: A fast and loop-free matlab implementation of surface finite elements. (*in preparation*), 2025.
- KLL19. B. Kovács, B. Li, and Ch. Lubich. A convergent evolving finite element algorithm for mean curvature flow of closed surfaces. *Numer. Math.*, 143:797–853, 2019.
- KLL20. B. Kovács, B. Li, and Ch. Lubich. A convergent algorithm for forced mean curvature flow driven by diffusion on the surfaces. *Interfaces Free Bound.*, 22(4):443–464, 2020.
- KLL21. B. Kovács, B. Li, and Ch. Lubich. A convergent evolving finite element algorithm for Willmore flow of closed surfaces. *Numerische Mathematik*, 149(4):595–643, 2021.
- KLLP17. B. Kovács, B. Li, Ch. Lubich, and C.A. Power Guerra. Convergence of finite elements on an evolving surface driven by diffusion on the surface. *Numer. Math.*, 137(3):643–689, 2017.
- Kov18. B. Kovács. High-order evolving surface finite element method for parabolic problems on evolving surfaces. *IMA J. Numer. Anal.*, 38(1):430–459, 2018.
- KP16. B. Kovács and C.A. Power Guerra. Error analysis for full discretizations of quasilinear parabolic problems on evolving surfaces. *NMPDE*, 32(4):1200–1231, 2016.
- LLRV09. B. Li, J. Lowengrub, A. Rätz, and A. Voigt. Geometric evolution laws for thin crystalline films: modeling and numerics. *Commun. Comput. Phys.*, 6(3):433–482, 2009.
- LMV13. Ch. Lubich, D.E. Mansour, and C. Venkataraman. Backward difference time discretization of parabolic differential equations on evolving surfaces. *IMA J. Numer. Anal.*, 33(4):1365–1385, 2013.
- LSU25. T. Laux, K. Stinson, and C. Ullrich. Diffuse-interface approximation and weak-strong uniqueness of anisotropic mean curvature flow. *European J. Appl. Math.*, 36(1):82–142, 2025.
- Lun95. A. Lunardi. *Analytic semigroups and optimal regularity in parabolic problems*. Modern Birkhäuser Classics. Birkhäuser/Springer Basel AG, Basel, 1995. [2013 reprint of the 1995 original] [MR1329547].
- Man12. C. Mantegazza. *Lecture Notes on Mean Curvature Flow*. Progress in Mathematics, Volume 290. Birkhäuser, Corrected Printing 2012.
- MS01a. K. Mikula and D. Sevcovič. Evolution of plane curves driven by a nonlinear function of curvature and anisotropy. *SIAM J. Appl. Math.*, 61(5):1473–1501, 2001.
- MS01b. K. Mikula and D. Sevcovič. Evolution of plane curves driven by a nonlinear function of curvature and anisotropy. *SIAM J. Appl. Math.*, 61(5):1473–1501, 2001.
- MS04. K. Mikula and D. Sevcovič. A direct method for solving an anisotropic mean curvature flow of plane curves with an external force. *Math. Methods Appl. Sci.*, 27(13):1545–1565, 2004.

- NO81. O. Nevanlinna and F. Odeh. Multiplier techniques for linear multistep methods. *Numerical Functional Analysis and Optimization*, 3(4):377–423, 1981.
- OOTT11. A. Oberman, S. Osher, R. Takei, and R. Tsai. Numerical methods for anisotropic mean curvature flow based on a discrete time variational formulation. *Commun. Math. Sci.*, 9(3):637–662, 2011.
- Poz07. P. Pozzi. Anisotropic curve shortening flow in higher codimension. *Math. Methods Appl. Sci.*, 30(11):1243–1281, 2007.
- Poz08. P. Pozzi. Anisotropic mean curvature flow for two-dimensional surfaces in higher codimension: a numerical scheme. *Interfaces Free Bound.*, 10(4):539–576, 2008.
- Poz12. P. Pozzi. On the gradient flow for the anisotropic area functional. *Math. Nachr.*, 285(5-6):707–726, 2012.
- Poz15. P. Pozzi. Computational anisotropic Willmore flow. *Interfaces Free Bound.*, 17(2):189–232, 2015.
- PPR14. R. Perl, P. Pozzi, and M. Rumpf. A nested variational time discretization for parametric anisotropic Willmore flow. In *Singular phenomena and scaling in mathematical models*, pages 221–241. Springer, Cham, 2014.
- PS04. P-O. Persson and G. Strang. A simple mesh generator in MATLAB. *SIAM Review*, 46(2):329–345, 2004.
- RT92. A. Roosen and J. E. Taylor. Simulation of crystal growth with faceted interfaces. *Mat. Res.Soc. Symp. Proc.*, 237:25–36, 1992).
- SSVW21. M. Salvalaglio, M. Selch, A. Voigt, and S. M. Wise. Doubly degenerate diffuse interface models of anisotropic surface diffusion. *Math. Methods Appl. Sci.*, 44(7):5406–5417, 2021.
- TCH92. J.E. Taylor, J.W. Cahn, and C.A. Handwerker. Overview no. 98 i—geometric models of crystal growth. *Acta Metallurgica et Materialia*, 40(7):1443–1474, 1992.